Comparing glucose acquisition strategies between two ancient fish species: lake sturgeon (*Acipenser fulvescens*) and North Pacific spiny dogfish (*Squalus suckleyi*)

By

Jenna M. Drummond

A Thesis submitted to the Faculty of Graduate Studies of

The University of Manitoba

in partial fulfilment of the requirements of the degree of

MASTER OF SCIENCE

Department of Biological Sciences

University of Manitoba

Winnipeg, Manitoba

Canada

Abstract:

The uptake of glucose within the gastrointestinal tract (GIT) is largely unexplored in ancient fish such as lake sturgeon (*Acipenser fulvescens*) and North Pacific spiny dogfish (*Squalus suckleyi*). Interestingly, within the GIT of Acipenserids (e.g. *A. fulvescens)* and Chondrichthyes (e.g. *S. suckleyi*) evolved an organ with scroll-like folds termed the spiral valve. Due to its structure, the spiral valve presumably slows down the passage of chyme and increases the gastrointestinal epithelial surface area to maximize nutrient absorption, suggesting it to be primarily responsible for nutrient acquisition. However, there is currently minimal functional data supporting this claim, and no data examining the effect of feeding state. Here, I aim to determine the functional role of the spiral valve in carbohydrate digestion and glucose acquisition during different feeding states and to determine if this role changes in organisms with different life histories. To test this, I assessed glucose digestibility and transport capacity along the GIT of *A. fulvescens* and *S. suckleyi* in fed and fasted fish. Digestibility was assessed through biochemical assays for the carbohydrate digesting enzyme maltase, while transport capacity was determined via i) mRNA abundance of the primary dietary glucose transporter (SGLT1), and ii) through *in vitro* intestinal fluxes. There were no significant postprandial changes in *sglt1* mRNA abundance in *A. fulvescens* in contrast to *S. suckleyi*, supporting their feeding strategies with *A. fulvescens* being continuous feeders and *S. suckleyi* being opportunistic feeders. In *S. suckleyi,* spiral valve *in vitro* glucose fluxes demonstrated changes in K_m and V_{max} in response to feeding, additionally supporting their opportunistic feeding strategy. The spiral valve played a primary role in glucose digestion and transport in *S. suckleyi*, whereas *A. fulvescens* utilized the anterior intestine in addition to the spiral valve. This demonstrates that the spiral valve may not always be the primary area of nutrient absorption as suggested by the literature, highlighting the importance of comparing morphological and functional studies. This study provides further insight into the functional role of the spiral valve in ancient fish along with increasing our understanding of the evolutionary history of glucose acquisition in vertebrates.

Acknowledgements:

First, I would like to thank Dr. Gary Anderson and Dr. Alyssa Weinrauch for providing me with great mentorship and for being lovely people. I aim to have a fraction of the kindness, patience, and consideration they demonstrate in their day-to-day lives. I would also like to thank my current and previous lab mates (in no particular order) for providing both emotional and technical support: Jess MacPherson, Tyler Edwards, Dr. Ian Bouyoucos, Ryan Wahl, Dr. Matt Thorstensen, Alex Schoen, Dr. Frauke Fehrmann, Ameera Kingra, Kaitlynn Weisgerber, Morgan Anderson, Dr. Lisa Hoogenboom, Alaina Taylor, Dr. Alison Loeppky, Dr. Will Bugg, and Dr. Gwangseok (Rex) Yoon. Honorary lab members that provided emotional support are Fergus Anderson, Yuuma Equus, and Jeremy Poortvliet.

I would like to acknowledge my committee members Dr. Dirk Weihrauch and Dr. Chengbo Yang for providing their insight towards this project. Thanks to the animal care staff at Bamfield Marine Sciences Centre and at the University of Manitoba for helping with the fish husbandry. The University of Manitoba campuses are located on original lands of Anishinaabeg, Cree, Oji-Cree, Dakota, and Dene peoples, and on the homeland of the Métis Nation. The water supplied at the University of Manitoba campuses is sourced from the Shoal Lake 40 First Nation. My work would be impossible without the land and water which it was conducted on. Funding was provided by the Natural Sciences and Engineering Research Council of Canada and Manitoba Hydro.

Lastly, thanks to my family for their unconditional love and support!

Dedication:

I would like to dedicate this thesis to Harry Styles, who released his album 'Harry's House' when I wanted to quit my degree and leave Winnipeg forever thus preventing me from following up on those plans.

Table of Contents:

List of Tables:

List of Figures:

List of Abbreviations:

ADP: adenosine diphosphate

ANOVA: analysis of variance

ATP: adenosine triphosphate

cDNA: copy deoxyribonucleic acid

DMSO: dimethyl sulfoxide

DNA: deoxyribonucleic acid

EDTA: Ethylenediaminetetraacetic acid

GAPDH: glyceraldehyde 3-phosphate dehydrogenase

GIT: gastrointestinal tract

GLUT: glucose transport protein

GLUT2: glucose transport protein-2

GLUT4: glucose transport protein-4

GPI: glucose phosphate isomerase

HK: hexokinase

MAPK: mitogen-activated protein kinase

mRNA: messenger ribonucleic acid

MS-222: tricaine methanesulfonate

NAD^+: nicotinamide adenine dinucleotide

NADES: natural deep eutectic solvent

NADH: nicotinamide adenine dinucleotide hydrogen

PFK1: phosphofructokinase-1

PGAM: phosphoglycerate mutase

PGK: phosphoglycerate kinase

PK: pyruvate kinase

RT-qPCR: real-time quantitative polymerase chain reaction

SEM: standard error of the mean

SGLT: sodium glucose linked transport protein

SGLT1: sodium glucose linked transport protein-1

SGLT2: sodium glucose linked transport protein-2

SGLT5: sodium glucose linked transport protein-5

SLC2: solute carrier family member 2

SLC5A: solute carrier family member 5A

TMAO: trimethylamine N-oxide

TPI1: Triose-phosphate isomerase-1

1.0.0 Introduction:

1.1.0 Glucose metabolism and energy balance:

Vertebrates are chemoheterotrophs; organisms that consume organic carbon sources, such as carbohydrates, to derive energy. Glucose is a ubiquitous critical energy source which is extracted from dietary carbohydrates through physical and chemical digestion. It is important for vertebrate metabolism and energy balance. As a result, most genes responsible for the metabolism of glucose are conserved amongst vertebrates (Zhang et al., 2018). The term "metabolism" describes the net anabolic and catabolic reactions that occur in the body; reactions which aim to either store or release energy through the conversion of metabolites into different forms depending on the energetic requirements of the organism. An example of an important glucose metabolic process is glycolysis, is a multistep reaction occurring in the cytoplasm of cells which utilizes the energy stored in glucose to produce the high-energy molecule ATP (Figure 1; Kumari, 2018). Pyruvate, a product of glycolysis, enters mitochondria and is utilized in the citric acid cycle for further ATP production in aerobic conditions. In anaerobic conditions, glucose and pyruvate are converted into lactate which additionally results in the production of ATP. Without glucose, glycolysis cannot occur which impedes on ATP production and on important metabolic pathways such as nucleotide (Lane & Fan, 2015) and lipid synthesis (Higgins et al., 1981) which utilize the intermediates and products of glycolysis. Glycolysis is one of the most ancient metabolic pathways (Canback et al., 2002); its conserved role throughout evolution shows the physiological importance of accessing the energy stored in glucose. However, the acquisition of glucose within the gastrointestinal tract is largely unexplored in phylogenetically ancient fish (Bucking, 2015; Leigh et al. 2017), leaving a gap in our knowledge about the evolution of glucose acquisition and energy balance in vertebrates.

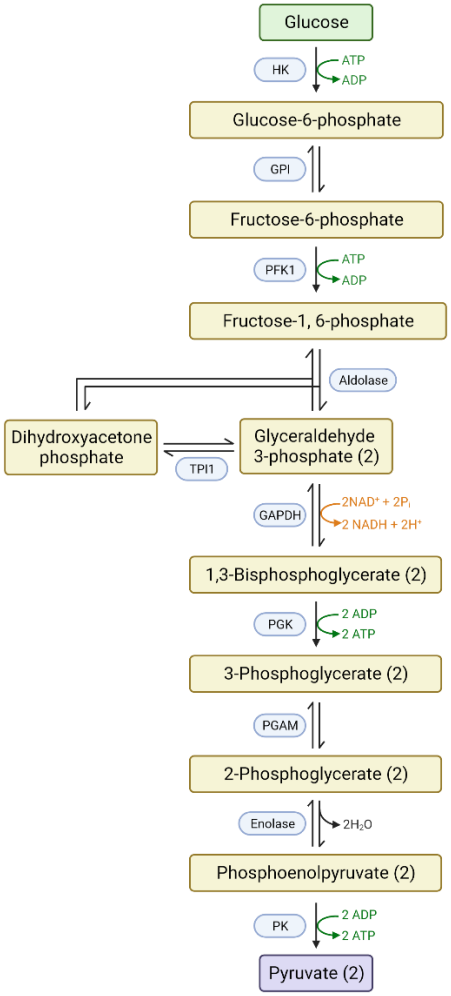

Figure 1: A schematic of the steps involved in glycolysis in which one glucose molecule results in the production of two molecules of pyruvate, two net molecules of ATP (adenosine triphosphate), two molecules of water, and two molecules of NADH (nicotinamide adenine dinucleotide hydrogen). Pyruvate may enter the citric acid cycle for further energy production. The precursors of ATP and NADH are, correspondingly, ADP (adenosine diphosphate) and NAD^+ (nicotinamide adenine dinucleotide). Blue circles indicate enzymes (HK: hexokinase; GPI: glucose phosphate isomerase; PFK1: phosphofructokinase-1; TPI1: Triose-phosphate isomerase-1; GAPDH: glyceraldehyde 3-phosphate dehydrogenase; PGK: phosphoglycerate kinase; PGAM: phosphoglycerate mutase; PK: pyruvate kinase). Yellow boxes indicate intermediates of glycolysis, and numbers in brackets indicate the number of molecules of the intermediate produced. This figure was created using BioRender.

1.2.0 Ancient fish evolutionary history:

To recognize the particular importance of glucose acquisition in ancient fish it is necessary to understand where they emerged in evolutionary biology. Approximately 400 million years ago the first jawed vertebrates diverged into Chondrichthyes (cartilaginous fish) and Osteichthyes (bony fish). Chondrichthyes is a monophyletic group that includes the subclass Elasmobranchii (sharks, skates, and rays) and Holocephali (Carrier et al., 2012). Osteichthyes are comprised of Actinopterygii (ray-finned fish), Sarcopterygii (lobe-finned fish) and basal Actinopterygii include the Acipenseriformes (sturgeon and paddlefish).

Acipenseriformes are classified as "living fossils" (Gardiner, 1984) due to their lack of morphological changes since their emergence in the fossil record over 200 million years ago (Patterson, 1982). Their slowed rate of molecular evolution also contributes to their "living fossil" status (Krieger & Fuerst, 2002); making them important organisms to study in evolutionary biology (Kaitetzidou et al., 2017). Similar to Acipenseriformes, Elasmobranchii additionally show slow mitochondrial DNA evolution rates (Martin, 1992). They also are the earliest known vertebrates with an acid secreting stomach (Smolka et al., 1994), making them relevant to understanding the evolution of the vertebrate gastrointestinal tract. Comparing the gastrointestinal physiological characteristics of two ancient fish, lake sturgeon (*Acipenser fulvescens),* and North Pacific spiny dogfish (*Squalus suckleyi)*, will increase our understanding of the functional evolution of the gastrointestinal tract.

1.3.0 Gastrointestinal tract form and function:

The process of glucose acquisition in vertebrates begins with dietary intake. The gastrointestinal tract (GIT; also referred to as the alimentary canal and digestive tract) is primarily responsible for food ingestion, physical and chemical digestion, and nutrient absorption. Particularly, the GIT is responsible for the acquisition of macromolecules: proteins, lipids, and carbohydrates. In brief, the GIT digests larger proteins into smaller molecules including amino acids, dipeptides, and tripeptides which are transported into gastrointestinal enterocytes through a suite of specific transport proteins (Karasov & Douglas, 2013). Lipid digestion primarily results in fatty acids, glycerol, monoglycerides, and lysophospholipids. Lipid transport is often mediated through the incorporation of the forementioned molecules into

micelles which can either passively diffuse or use transport proteins (particularly for short-chain fatty acids) to cross the hydrophobic plasma membrane (Karasov & Douglas, 2013). Oligosaccharides and disaccharides present in chyme are broken down into monosaccharides, including D-galactose, D-fructose, and D-glucose, through physical and chemical digestion within the GIT (Hediger & Rhoads, 1994). The breakdown and subsequent uptake of carbohydrates will be explored later.

Intra- and interspecific GIT morphological differences exist partly due to variations in diet and feeding strategy of the organism (Elliot & Bellwood, 2003; Olsson et al., 2007; Redjadj et al., 2014). Despite the vast differences in feeding strategies amongst elasmobranchs, they share a relatively anatomically similar GIT (Bucking, 2015) which resembles that of Acipenseriformes (Wegner et al., 2009). However, an exception is that Acipenseriformes have an additional structure called the pyloric ceca. This structure is a series of blind sphincterless ducts that increase the gastrointestinal surface area and is located between the stomach and intestine (Buddington & Diamond, 1987). The pyloric ceca's epithelial layer is similar to the intestine (Buddington & Diamond, 1987) and is a structure that is also found in teleosts with quantity and morphology ranging broadly between species (ranges from 0 to over 1000; Hossain & Dutta; 1996). The pyloric ceca may appear tassel-like in fish that have many ceca (Wilson & Castro, 2010), alternatively, in species with a lower number of ceca (e.g. Acipenseriformes), the ceca combine together into a single compact organ.

Outside of the pyloric ceca, the GIT of ancient fish includes the mouth, pharynx, esophagus, stomach, anterior intestine (proximal intestine), spiral valve (scroll valve/spiral intestine), and colon (distal intestine/rectum). The mouth and pharynx obtain food from the external environment. Mechanical and chemical digestion begins once food enters the mouth through the action of teeth and salivary amylase; food is then delivered to the stomach via the esophagus (Wilson & Castro, 2010). The stomach stores food and utilizes mechanical and chemical digestion; chemical digestion occurs primarily through secretions of gastric acid and the protease zymogen, pepsinogen (protein digestion). In most fishes with a stomach there are two distinct sections: the anterior descending cardiac stomach and the posterior ascending pyloric stomach (Wegner et al., 2009; Wilson & Castro, 2010). The cardiac stomach primarily acts as a food storage section and the pyloric stomach is the secretory section of the stomach

(Bakke et al., 2010); it is separated from the anterior intestine by the pyloric sphincter (pyloric valve; Bucking, 2015; Wegner et al., 2009).

All intestinal sections (anterior intestine, spiral valve, and colon) function to complete digestion and to absorb nutrients. The anterior intestine has a folded surface to increase its surface area (Chatchavalvanich et al., 2006) and is closely associated with the pancreas and liver (Bucking, 2015). The pancreas produces enzymes that aid in digestion, and the liver produces bile; the products of the pancreas and the liver are secreted into the anterior intestine to create a favorable environment for digestion of macromolecules. Unlike elasmobranchs with a compact mammalian-like pancreas, Acipenseridae have a diffuse pancreas (Daprà et al., 2009; Jönsson, 1991, Vajhi et al., 2013). It should be noted that the anterior intestine in *A. fulvescens* is much larger than *S. suckleyi* who have a very short anterior intestine (Figure 2). Following the anterior intestine is the spiral valve. Interestingly, the suggested primary site for digestion and nutrient absorption, and therefore glucose uptake, in ancient fish is the spiral valve (Bucking, 2015; Jhaveri et al. 2015; Venero et al, 2015) which is analogous to the primary nutrient absorption site in mammals, the small intestine (Theodosiou & Oppong, 2019).

The spiral valve is a plesiomorphic GIT morphological feature that emerged early in the evolution of vertebrates (Argyriou et al. 2016); unique to non-tetrapod Sarcopterygii, non-teleost Actinopterygii and Chondrichthyes (Wilson & Castro, 2010). The spiral valve contains scroll-like folds that presumably slow down the passage of chyme and increase the mucosal surface area for nutrient absorption (Bakke et al., 2010; Buddington & Christofferson, 1985). Increased transit time subsequently increases opportunities for chyme to encounter digestive enzymes and mucosal absorptive sites. The mucosal surface area of the spiral valve is increased since the morphology of its folds includes a double layered epithelium with a shared submucosa, enabling chyme to be absorbed from both sides of its folds (Hassanpour & Joss, 2009). Ancient fish have a shortened GIT; the increased digestive surface area of the spiral valve and its highly developed surface area is thought to compensate for this shortened length (Theodosiou & Oppong, 2019; Venero et al. 2015; Wilson & Castro, 2010).

Posterior to the spiral valve is the colon. Longitudinal rugae are present in the colon in Acipenseridae suggesting an absorptive function (Buddington & Christofferson, 1985). Finally, the colon opens to the cloaca where excreta is released to the external environment.

1.3.1 Functional regionality within the intestine:

Along the small intestine in mammals are regions with morphological and functional differences (duodenum, jejunum, and ileum). This functional regionality has been described in the fish intestine. For example, a proximal to distal gradient of nutrient absorption has been demonstrated in the GIT of teleosts (Bakke-McKellep et al., 2000; Hernandez-Blazquez et al., 2006; Krogdahl et al., 1999), however, it should be noted that these gradients can vary between species (Buddington et al., 1987; Krogdahl et al., 1999). Like teleosts, functional regionality within the ancient fish intestine has been suggested. For example, the spiral valve in little skate (*Leucoraja erinacea*) has histochemical and functional regionality in the expression of acid mucin goblet cells; expression in the anterior to mid spiral valve is similar to the mammalian small intestine and the distal region has expression levels similar to the mammalian colon (Theodosiou et al., 2007; Theodosiou & Oppong, 2019). Similarly, regional morphology has been suggested in the spiral valve of Gulf of Mexico sturgeon (*Acipenser oxyrhynchus*) where there were 50% fewer and shorter folds in the posterior region, suggesting an increased role in nutrient absorption in the anterior section (Venero et al., 2015). Furthermore, Australian lungfish (*Neoceratodus forsteri*) has increased surface area in the anterior spiral valve indicative of increased potential for nutrient absorption (Hassanpour & Joss, 2009). It should be noted that the above examples from the literature regarding ancient fish do not include intestinal regional differences of carbohydrate digestion and uptake.

By making functional comparisons along the intestine of *A. fulvescens* and *S. suckleyi,* I can determine if there is regionality in the digestion and acquisition of carbohydrates. The anterior intestine of teleost fish has high glycolytic potential and high levels of glucose storage; making it important for regulating postprandial glucose homeostasis (Chen et al., 2017). Similarly, the early to mid small intestine are primarily responsible for sugar uptake in mammals (Wright et al. 2003). Therefore, it can be hypothesised that its analogue in ancient fish, the anterior intestine and anterior spiral valve, play a primary role in glucose acquisition.

1.4.0 Gastrointestinal mucus:

Once food enters the GIT it encounters a layer of mucus surrounding the epithelial cells lining the GIT. Gastrointestinal mucus produced by goblet cells protects epithelial cells from mechanical and chemical harm and has an immunological function. There are differences in mucus composition (Johansson et al., 2011; Rodríguez-Piñeiro et al., 2013) and thickness (Atuma et al., 2001) along the gastrointestinal tract of mammals suggesting mucus specialization along the tract. A factor that contributes towards differences in mucus composition includes mucins. Mucins are large glycoproteins that, in the GIT, form mucus and the glycocalyx and can be either membrane bound or secreted. Genomic analysis suggests that transmembrane mucins appeared in vertebrates and that gel-forming mucins appeared in invertebrates suggesting different functional roles for gel-forming and transmembrane mucins (Lang et al., 2007). The transmembrane mucin family has expanded in higher vertebrates indicating the importance and increased diversity in function of these mucins (Lang et al., 2004). Overall, the expanding specialization of mucins indicates the relevance of the functional role of mucus in the GIT.

Mucus may also have a significant role in aiding digestion. Due to its chemical composition mammalian gastrointestinal mucus is proposed as being a natural deep eutectic solvent (NADES) (Van Kempen & Boerboom, 2023). NADES matrices support enzyme activities and can solubilize carbohydrates which do not dissolve in water or lipids. Hence, Van Kempen and Boerboom (2023) suggest that starch is dissolved by the mucosal NADES matrix, and subsequently enzymatically broken down and absorbed by enterocytes. If fishes have a similar mucosal layer, then perhaps this mucosal digestion and absorption occurs for carbohydrates, subsequently aiding the digestive tract in acquiring carbohydrates.

1.5.0 Enzymes and carbohydrate digestion:

Digestive enzymes assist in chemically digesting food into components that may be transported across the epithelium of the GIT. Fish have demonstrated the capability of transporting the monosaccharides glucose, fructose, galactose, and N-acetyl-glucosamine (product from the breakdown of chitin; Clements & Raubenheimer, 2006). Within the GIT, dietary carbohydrates are hydrolyzed into monosaccharides through physical digestion, and chemical digestion by pancreatic enzymes and brush-border hydrolases (Hediger & Rhoads

1994). Ancient fish utilize the enzymes chitinase and α-amylase to initially break down carbohydrates. Chitinases break down chitin (found in the exoskeleton of arthropods) and have been found in the colon of elasmobranchs (Fänge et al., 1979; Jhaveri et al., 2015). Along with chitin, other dietary carbohydrates include starch and glycogen. Starch and glycogen are primarily hydrolyzed by α-amylase to produce maltose and oligosaccharides. In fish, α-amylase primarily hydrolyzes glycogen since starch is an uncommon dietary component (Bakke et al., 2010). There is a high level of molecular conservation amongst fish amylases, which underscores their importance in carbohydrate digestion (Krogdahl et al., 2005). For transport across the gastrointestinal epithelium the products of carbohydrases are further hydrolyzed by disaccharidases like maltase, which are present in the brush border of the GIT epithelium (Bakke et al., 2010). The enzyme maltase converts the larger disaccharide maltose into the more easily transported monosaccharide glucose within the lumen of the GIT.

There is limited research on the functional regionality of enzyme activity along the GIT of both elasmobranchs and acipenserids (Bucking, 2016; Nevalenny & Bednyakov, 2017; Leigh et al., 2017). From my understanding, the regionality of digestive enzyme activity has only been determined in Russian sturgeon (*Acipenser gueldenstaedtii*; Nevalenny & Bednyakov, 2017) and bonnethead sharks (*Sphyrna tiburo*; Jhaveri et al., 2015) and neither study contained a component comparing the fishes' feeding states. Increased enzyme activity indicates increased digestion and faster food processing (Jhaveri et al., 2015). Therefore, examining regional digestive enzyme activities indicates the primary areas of carbohydrate digestion. The determination of regional enzyme activity in *A. fulvescens* and *S. suckleyi* will increase our understanding of ancient fish digestive enzymes.

1.5.1 Maltase:

Maltase is present in acipenserids (Buddington, 1985; Buddington & Doroshov, 1986; Hung et al., 1989) and elasmobranchs (Jhaveri et al., 2015) making it a good enzyme to compare between *A. fulvescens* and *S. suckeyi*. By analyzing and comparing maltase activity throughout the GIT in ancient fish species, this study aims to identify the primary sites where carbohydrates are hydrolyzed into monosaccharides for absorption by the GIT in these fish. Other studies have been conducted determining the regionality of maltase activity along the GIT in both carnivorous

and herbivorous fish. For example, Harpaz and Uni (1999) found that maltase activity was significantly highest in the midgut of omnivorous tilapia hybrids (*Oreochromis niloticus*×*Oreochromis aureus*) and herbivorous silver carp (*Hypophthalmichthys molitrix*) with the carnivorous hybrid striped bass (*Morone saxatilis*×*Morone chrysops)* having significantly lower activity in comparison. Interestingly, the pyloric ceca had lower maltase activity than the other intestinal sections examined. Alternatively, the pyloric ceca had the highest relative contribution of maltase along the gastrointestinal tract in the Atlantic salmon (*Salmo salar L.;* Krogdahl & Bakke-McKellep, 2005*)*. The zonation of metabolic enzyme activities varies among teleost species, making it challenging to draw generalizations about teleosts (Mommsen et al., 2003). As the suggested primary site for digestion and nutrient absorption in ancient fish is the spiral valve (Bucking, 2015; Jhaveri et al. 2015; Venero et al., 2015), it is predicted that the highest activity level of maltase would occur in the spiral valve. However, further investigation is needed to determine if there is additional regional expression within this structure.

1.6.0 Transport proteins and carbohydrate acquisition:

After glucose is derived from dietary carbohydrates from the activity of pancreatic enzymes and brush border hydrolases, it is transported across the GIT epithelium. In the small intestine of mammals, glucose is either absorbed paracellularly across tight junctions or transcellularly through membrane bound proteins (Pessin & Bell, 1992). Since glucose is a hydrophilic molecule, its transport from the lumen of the digestive tract into gut enterocytes needs to be facilitated by membrane bound transport proteins. There are two types of known glucose transport proteins: glucose transport proteins (GLUTs) and sodium glucose linked transport proteins (SGLTs). SGLTs are members of the SLC5A (solute carrier family member 5A) family (Wright & Turk, 2004), and GLUTs are members of the SLC2 (solute carrier family member 2) family (Uldry & Thor, 2004). GLUTs and SGLTs are both key glucose transporters present in the GIT of vertebrates (Hediger & Rhoads 1994; Yoshikawa et al. 2011). Outside of their role in nutrient uptake, SGLT and GLUT isoforms SLGT1 and GLUT2 have additionally been suggested to play a role in glucose sensing in mammals (see below; Röder et al., 2014).

GLUT isoforms have been identified in almost all cell types, whereas SGLTs are primarily found in tissues responsible for glucose recovery, including the small intestine and

kidney (Pessin & Bell, 1992). There are thirteen known isoforms of GLUT in humans; the variety of GLUT isoforms with different kinetic and biochemical properties allows for optimal glucose uptake in different tissues under various physiological conditions (Pessin & Bell, 1992). It is suspected that ancient fish have fewer isoforms due to their early emergence in the evolution of glucose metabolism; only three potential GLUT isoform sequences have been currently identified in the transcriptome of elasmobranchs and there has been limited research on their tissue distribution (Deck et al., 2016). SGLT transport proteins are generally considered well conserved (Liang et al., 2021).

1.6.1 Apical membrane glucose transport:

Sodium glucose linked transporter-1 (SGLT1; encoded by SLC5A1) is a key glucose transport protein present in the GIT of all vertebrates thus far examined, responsible for transporting glucose across the apical membrane of enterocytes lining the GIT (Suzuki et al., 2001; Yoshida et al., 1995). In mammals, SGLT1 is concentrated in the brush border membrane of the small intestine and in the proximal tubule of the kidney (Hediger et al., 1989). It should be noted that renal apical glucose transport additionally occurs though SGLT2 (Ghezzi et al., 2018). It has been suggested that SGLT1 does transport glucose alone and may work in conjunction with additional low-affinity passive glucose transporters on the apical membrane of gastrointestinal enterocytes; either GLUT2 (rapidly trafficked to the plasma membrane when needed; Kellett, 2001) or another SGLT isoform (Wright et al., 2003). Naftalin (2014) suggests that apical GLUT2 could additionally serve an osmoregulatory function to mitigate enterocyte volume changes with intracellular glucose uptake. Interestingly, GLUT2 knockouts in mice did not impact apical intestinal glucose uptake in comparison to control mice (Stümpel et al., 2001) which has caused speculation about their significance in apical glucose uptake. However, apical GLUT2 has not been established in fish as current research has primarily been conducted on mammals (Cohen et al., 2014; Kellett 2001). Some fish may not even use the isoform GLUT2; in *S. suckleyi* Deck et al. (2016) found absence of *glut2* mRNA transcripts but did find the presence of *glut4* transcripts. This led to the suggestion that GLUT4 in elasmobranchs may function as the glucose transport protein across the basolateral membrane. In contrast the apically present SGLT1 has been well established in fish (Maffia et al., 1996; Polakof et al., 2012; Sala-Rabanal et al., 2004).

SGLT1 is a high-affinity, low-capacity symport which requires ATP to couple glucose transport against its concentration gradient with the transport of sodium down its electrochemical gradient across the apical membrane of the intestinal epithelium (Figure 2; Sano et al., 2020). Glucose transport is dependent on sodium ions in which the binding of two sodium ions induces a conformational change in the transport protein to allow glucose to bind; the two sodium ions and glucose are subsequently transferred across the plasma membrane and deposited into the cytoplasm of gut enterocytes (Wright et al., 2003). Though glucose transport is dependent on sodium, other cations such as hydrogen and lithium may replace sodium; however, these alternative cations have a lower affinity to glucose (Wright et al., 2003). Once glucose enters the cell, hexokinase can phosphorylate glucose to form glucose-6-phosphate (G6P), which prevents glucose from leaving the cell (Gamperl & Driedzic, 2009), or glucose can diffuse across the basolateral membrane into the blood to be utilized by other cells in the body. Sodium-potassium ATPases in the basolateral membrane also pump sodium out of the cell to maintain the inward gradient of sodium required for SGLT1 to transport glucose inside the cell (Hediger & Rhoads 1994).

Within the intestine, SGLT1 transports the sugars glucose and galactose, as well as glucose analogs (e.g., α-methyl-D-glucopyranoside) that cannot be metabolized; however, it does not transport fructose, which is alternatively passively transported across the apical membrane by SGLT5 in mammals (Wright et al., 2003). Though SGLT1 is primarily regarded for transporting sugars, it has demonstrated additional functions. SGLT1 has suggested involvement in gastric motility; for example, phlorizin inhibited SGLT1 in rats, reducing the glucose-dependent inhibition of gastric motility (Raybould et al., 1995). Rabbit SGLT1 expressed in *Xenopus laevis* oocytes acted as a sodium independent urea channel (Leung et al., 2000). Alongside urea, SGLT1 has also acted as a functional water channel (Loo et al., 2002; Zeuthen et al., 2016). There is also evidence of water transport through SGLT1 independent of sodium and glucose (Wright et al., 2017). In fact, Zeuthen et al. (2016) suggests that 60-70% of passive water transport in the mouse intestine is mediated by on SGLT1. Though less studied in fish, the multifunctional nature of these transport proteins may compound their use in the fish gastrointestinal tract, especially for elasmobranchs which utilize urea for osmoregulation (Smith, 1936; Speers-Roesch & Treberg, 2010).

Regionality in SGLT1 expression has been shown in teleosts. For example, *sglt1* mRNA expression in common carp (*Cyprinus carpio*; Syakuri et al., 2019) and rainbow trout (*Oncorhynchus mykiss*; Kamalam et al., 2013) decreases from the anterior to posterior section of the intestine. The gilthead sea bream (*Sparus aurata*) also has a higher *sglt1* expression in the proximal intestine in comparison to the distal intestine (Sala-Rabanal et al., 2004). This makes it likely that SGLT1 expression could also be highest in the anterior portion of the intestine (anterior intestine and anterior spiral valve) in *A. fulvescens* and *S. suckleyi*.

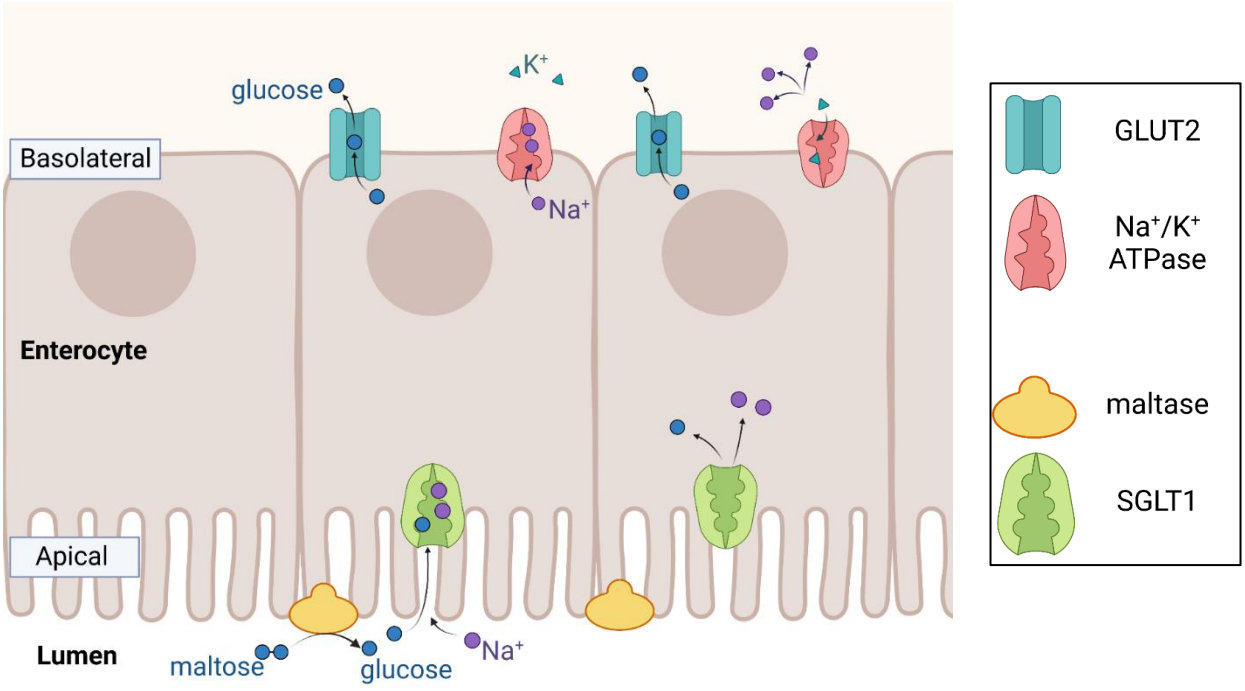

Figure 2: Simplified diagram of glucose transport across the apical and basolateral membrane of vertebrate gastrointestinal enterocytes (best characterized in mammals). Sodium glucose linked transport protein-1 (SGLT1) is depicted by the green transport proteins on the apical membrane. On the basolateral membrane: glucose transport protein-2 (GLUT2) is illustrated by the blue transport proteins and sodium-potassium ATPase is represented by the red transport proteins. The brush border enzyme maltase is depicted by the yellow proteins. This figure was created using BioRender.

1.6.2 Basolateral membrane glucose transport:

After passage across the apical enterocyte plasma membrane, glucose may be used as a fuel source for enterocytes or pass through the basolateral membrane for usage in other areas of the body (Wright et al., 2003). Glucose transport protein-2 (GLUT2) is a uniporter that uses facilitated diffusion to transport glucose across the basolateral membrane down its concentration gradient (Figure 2). GLUT2 additionally transports fructose, mannose and galactose across the basolateral membrane (Castillo et al., 2009; Cheeseman, 1993) and is typically expressed in the liver, pancreas, and intestine in mammals (Pessin & Bell, 1992).

Castillo et al. (2009) compared zebrafish, Atlantic cod, rainbow trout and human GLUT2 and determined that GLUT2 is well conserved after fish and mammals diverged. It can be argued that there is a high level of conservation over evolutionary time, as evidenced by the presence of mammalian SGLT1-like and GLUT2-like transport proteins in the apical and basolateral membrane of the midgut in the parasitoid wasp, *Aphidius ervi* (Caccia et al., 2007). However, this may not be the case amongst non-teleost fish. In the *S. suckleyi* transcriptome, it has previously been determined that there is an absence of *glut2* (Deck et al., 2016). GLUT2 and GLUT4 are thought to be duplications of each other; in tissue mRNA analysis of *S. suckleyi*, *glut4* was expressed in the liver and intestine instead of *glut2*, suggesting that the diversity of GLUT2 functionality has been lost in elasmobranchs (Deck et al., 2016). In mammals, GLUT4 is present in fat and skeletal muscle cells and is regulated by insulin, which signals for GLUT4 within intracellular vesicles to be trafficked to the plasma membrane to enable glucose uptake (Stöckli et al., 2011). From my knowledge, there currently are no functional studies examining the role of intestinal GLUT4 in elasmobranchs.

1.7.0 Ancient fish and carbohydrates:

As ectotherms, fish have lower metabolic rates compared to endotherms, which may result in decreased glucose uptake requirements (Ferraris et al., 1989). Both elasmobranchs (Ballantyne, 1997), and acipenserids (Hung et al., 1989) have demonstrated the ability to digest carbohydrates. Despite this capability, it is important to note that fish species vary in their ability to utilize different carbohydrate sources (Hung, 1991; Millikin, 1982). For example, acipenserids can obtain energy from the monosaccharide glucose more effectively than plant-based polysaccharides (i.e. fructose, cellulose, and starch; Hung et al. 1989). Since they are carnivorous

fish, they do not typically consume plant-based polysaccharides and therefore likely have less architecture present to effectively digest and transport these carbohydrates. This difference in the ease of carbohydrate utilization among different species is likely determined by gastrointestinal morphological and biochemical variations. Dietary carbohydrate content in a fish's natural diet impacts its intestinal capacity for glucose acquisition (Buddington et al., 1987). However, after examination of digestive enzyme activities in closely related prickleback species with different diets (carnivorous and herbivorous), it was suggested that phylogeny can sometimes play a more significant role than diet in the process of digestion (Chan et al., 2004; German et al., 2004). For example, Chan et al. (2004) found that the carnivorous *Xiphister atropurpureus* exhibited similar α-amylase activity to its herbivorous sister species *Xiphister mucosus,* in comparison to the more distantly related carnivorous *Anoplarchus purpurescens* which had relatively lower levels of amylase activity. Diet also influences gastrointestinal morphology. For example, Olsson et al., (2007) demonstrated adaptive plasticity in the gut length of Eurasian perch (*Perca fluviatilis*) by feeding them different food types.

Due to the carnivorous nature of ancient fishes, carbohydrates are typically not the primary component of their diet. For example, though elasmobranchs have a large range of diets and feeding strategies, they are primarily carnivorous and typically feed on protein and fat rich meals (Leigh et al., 2017). Additionally, adult sturgeon primarily consume fats and proteins due to their carnivorous lifestyle, with a diet primarily composed of invertebrates and fish (Buddington & Christofferson, 1985). Despite this, white sturgeon (*Acipenser transmontanas*) fed different carbohydrate diets maintain consistent plasma glucose levels, suggesting that they have adequate mechanisms to maintain glucose homeostasis (Hung et al., 1989). Though ancient fish are primarily carnivorous, their diet may occasionally include carbohydrate rich meals (Venero et al., 2015). For example, mollusc consumption enables access to generous stores of the energy rich carbohydrate glycogen (Darriba et al., 2005). Aside from its role in energy balance, glucose has been suggested to be involved in signalling for the inhibition of gastric emptying (Raybould & Zittel, 1995). Höfer et al. (1999) suggest that only carbohydrates are able to induce chemosensory reactions in enterocytes. Despite being less prevalent than lipids and proteins in the ancient fish diet, the various gastrointestinal physiological roles of carbohydrates deem them worth investigating in ancient fish.

1.7.1 Alternative energy sources:

Other energy sources exist besides carbohydrates. Mammals use ketone bodies (high-energy compounds produced by the liver) peripherally as an alternative energy source when glucose availability is limited (Laffel, 1999). Alternatively, elasmobranchs rely on ketone bodies over glucose as an oxidative fuel; it has been proposed that this is related to their need to produce urea for their urea-dependent method of osmoregulation (Speers-Roesch & Treberg, 2010). It should be noted that carbohydrates are still utilized as an energy source in elasmobranchs, despite reduced plasma glucose levels in comparison to teleosts of a similar size and metabolic rate (Polakof et al., 2011).

Fasted fish typically maintain their plasma glucose levels similar or slightly lower than satiated individuals likely through depletion of hepatic glycogen stores (Navarro and Gutiérrez, 1995). As a result, maintenance of plasma glucose levels reinforces its physiological importance (Polakof et al., 2011). However, one exception is the small-spotted catshark (*Scyliorhinus canicular*): it has previously been demonstrated to have plasma glucose levels decrease to a minimum of 0.03 mM eight days post-feeding and only return to baseline levels (0.67 mM) after 2 months of fasting (Navarro and Gutiérrez, 1995). This further supports the reduced reliance on glucose as an energy source in elasmobranchs. It is interesting to compare an ancient fish that may use ketone bodies as a preferential energy source (*S. suckleyi*) with one that has an increased reliance on glucose as an energy source (*A. fulvescens).*

1.8.0 Physiological responses to feeding state:

The gastrointestinal tract is energetically expensive to maintain. For example, the comparison of sheep, rats, mice, cattle, and chicken studies led Cant et al. (1996) to conclude that the gastrointestinal tract utilizes approximately 20% of incoming energy, making it a very metabolically active system. To conserve energy, some species have developed mechanisms to up or down regulate different gastrointestinal mechanisms to adapt to different feeding states. For example, by analyzing various snake species it was determined that the feeding strategy of consuming large infrequent meals contributes towards a large postprandial physiological response in comparison to relatively frequently feeding snakes (Secor & Diamond, 1995; Secor & Diamond, 1998). These large postprandial responses were impressive, for example the mass of

the small intestine in Burmese pythons increased 40% within 6 hours of feeding (Secor & Diamond 1995). Though the metabolic costs are large during feeding for individuals that downregulate various gastrointestinal mechanisms, this downregulation is thought to contribute towards net energetic savings due to lower energetic costs towards maintaining the intestine during fasting periods (Secor & Diamond, 1995; Secor & Diamond, 1998). Gastrointestinal histochemical responses in fasting fish are similar to reptiles and amphibians (Zaldúa & Naya, 2014).

The natural environment of many fish results in periods of food deprivation (Furné & Sanz, 2018). A variety of physiological changes have been shown in fasted fish including decreased metabolic rate (Binner et al., 2008) and decreased blood glucose levels (Furné et al., 2012). Additionally, *S. trutta* (brown trout) glucose uptake in white and red muscle in response to a glucose load was ~50% higher in fed fish in comparison to their fasted counterparts (Blasco et al., 1996). A variety of studies have been conducted regarding gastrointestinal physiological changes occurring during periods of both long- and short-term food deprivation in fish. For example, gastrointestinal morphological changes were shown when intestinal and microvilli surface area was reduced in starved (150 days food withheld) vermiculated sailfin catfish (*Pterygoplichthys disjunctivus;* German et al., 2010). Gastrointestinal tissue mass and digestive enzyme activities decreased with fasting in Atlantic salmon (*Salmo salar;* Krogdahl & Bakke-McKellep, 2005). A five day fast in Nile tilapia (*Oreochromis niloticus*) also subsequently altered the distribution and increased the activity of metabolic enzymes (Mommsen et al., 2003). Starved fish also had a decreased capacity to digest macronutrients in Adriatic sturgeon (*Acipenser naccarii*) and rainbow trout (*Oncorhynchus mykiss*; Furné et al., 2008). The above examples demonstrate that morphological, biochemical, and intestinal regional differences may result in response to feeding state.

Intestinal physiological responses (i.e. enzyme activity and transporter expression) typically are shown to reflect the frequency of feeding in fish (Bucking 2015). The digestive capabilities of intermittent feeding sharks may be up- or down- regulated in comparison to continuous feeders whose GIT is continually ready to digest food (Papastamatiou & Lowe, 2005). For example, *S. suckelyi* intestinal *glut4* expression was significantly higher in fed fish in comparison to their fasted counterparts (Deck et al., 2016). Therefore, physiological differences

may be encountered in the opportunistic infrequent feeding *S. suckleyi* in comparison to the more continuously feeding *A. fulvescens.*

1.9.0 Thesis objectives:

The gastrointestinal tract (GIT) is responsible for food ingestion, physical and chemical digestion, and nutrient absorption. The spiral valve is found in the GIT of non-tetrapod lobe-finned fish (Sarcopterygii), non-teleost ray-finned fish (e.g. Acipenseriformes), and cartilaginous fish (Chondrichthyes; Argyriou et al., 2016; Wilson & Castro, 2010). It is a portion of the intestine that contains folds which presumably slow down the passage of chyme, increasing the time available for digestion and subsequent nutrient absorption (Bakke et al., 2010; Buddington & Christofferson 1985). These folds also function to increase the available surface area for nutrient absorption while maintaining the overall length of the intestine. Due to the structure of the spiral valve, it has been suggested as the primary area of nutrient absorption in the GIT (Bucking, 2015; Venero et al., 2015). However, there is currently a lack of functional data regarding its digestive and transport properties to support this claim. By examining the spiral valve's digestive and absorptive properties in a representative non-teleost ray-finned fish, such as *Acipenser fulvescens* (lake sturgeon), and a cartilaginous fish, such as *Squalus suckleyi* (North Pacific spiny dogfish) this study provides a greater understanding of the functional role of the spiral valve in ancient fishes.

This study aims to increase our understanding of the relative role of the spiral valve in nutrient acquisition by examining its capacity to break down and absorb glucose, a ubiquitous energy source, in comparison to other gastrointestinal regions (Figure 3). Since different physiological mechanisms may be up- and/or downregulated according to metabolic state, the gastrointestinal tract was examined at multiple postprandial timepoints. The comparison of two phylogenetically distant organisms (*A. fulvescens* and *S. suckleyi*) that both have a spiral valve (Figure 3) can help us begin to elucidate if the role of the spiral valve in glucose acquisition is conserved. These research aims were accomplished through anterior to posterior examination of the GIT in each species. Specifically, I assessed:

1. Regional activity of the enzyme maltase
2. Regional abundance of the glucose transporter *sglt1* mRNA transcripts
3. Michaelis-Menten kinetics of glucose transport (intestinal regions only)

The determination of regional maltase activities and *sglt1* transcript abundance patterns during a postprandial timeseries will allow me to test the hypothesis that the GIT of ancient fish has regional separation for carbohydrate digestion and glucose acquisition. Since the suggested primary site for digestion and nutrient absorption in ancient fish is the spiral valve (Bucking, 2015; Jhaveri et al. 2015; Venero et al., 2015), it can be predicted that the highest activity level of maltase and the highest transcript abundance of *sglt1* will occur in the spiral valve of both species of fish. The impact of a postprandial timeseries on maltase activity, *sglt1* transcript abundance, and the functional transport capacity of glucose in the intestine of *A. fulvescens* and *S. suckleyi* will additionally allow me to test the hypothesis that mechanisms of digestion and glucose acquisition in ancient fish are impacted by feeding strategy. *S. suckleyi* opportunistically feed in opposition to *A. fulvescens* which continually feed, therefore I expect *S. suckleyi* to down-regulate digestive and uptake mechanisms more readily during fasting periods.

Glucose acquisition within the GIT is largely unexplored in phylogenetically ancient fish such as *A. fulvescens* and *S. suckleyi* (Bucking, 2015; Leigh et al. 2017), leaving a gap in our knowledge regarding the evolution of glucose acquisition in vertebrates. By understanding glucose uptake in ancient fish with different feeding strategies like the continuously feeding *Acipenser fulvescens* and the opportunistically feeding *Squalus suckleyi* insight is given towards the evolution of uptake of an important nutrient involved in one of the most ancient metabolic pathways. This study provides further insight towards understanding the evolutionary significance of the emergence of the spiral valve along with increasing our understanding of its role in the digestion and absorption of nutrients.

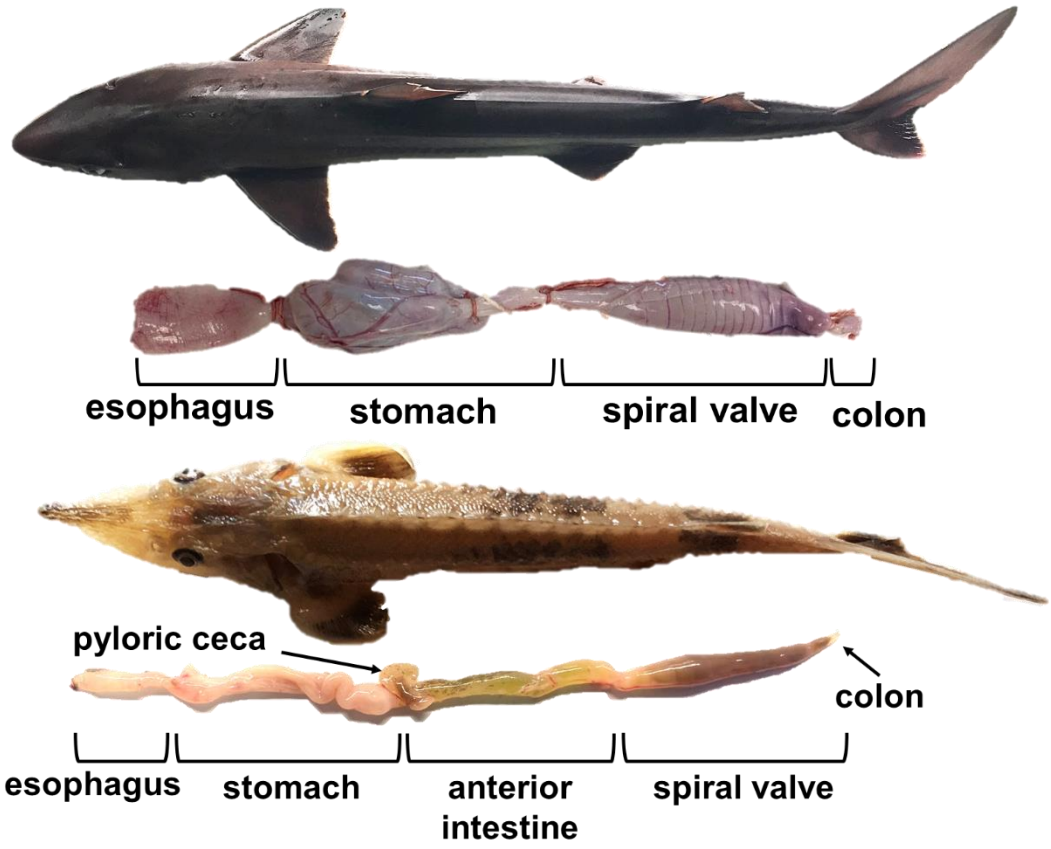

Figure 3: Gastrointestinal morphology of *S. suckleyi* (top) and *A. fulvescens* (bottom). Note that these images are not to scale.

2.0.0 Methods:

2.1.0 Animal husbandry and feeding protocols:

2.1.1 *Acipenser fulvescens:*

Lake sturgeon (*Acipenser fulvescens)* gametes were collected from wild spawning adults at Point du Bois, Manitoba under provincial collection permit #22554910. Gametes were manually fertilized and reared at the University of Manitoba hatchery. Twenty-eight one-year-old *A. fulvescens* (50.3 ± 2.8 g) held in 60-gallon flow-through tanks at 16 ± 1°C were utilized for determining enzymatic activity and transport protein transcript abundance. Twenty-eight two-year-old *A. fulvescens* (169.6 ± 8.3 g) held in 600-gallon recirculating tanks at 16 ± 1°C were used for *in vitro* fluxes. One-year-old fish were not used for *in vitro* experimentation due to having insufficient gastrointestinal tissue quantity (Table 1). All *A. fulvescens* used were offered

~2% of the total tank body mass daily of commercial pellet (#11700995; Bio-Oregon, Vancouver, Canada) and fed until satiation. Fish were removed for tissue sampling and experimentation at the following post-feeding timepoints: 6 hours (6 h 16 min ± 9 min), 24 hours (24 h 35 min ± 6 min), 96 hours (96 h 37 min ± 11 min), and 7+ days (8-10 days). However, the 96-hour post-feeding timepoint was only used for determining enzymatic activity and transport protein transcript abundance due to having limited amounts of ^{14}C-glucose. I used the enzymatic activity and transport protein transcript abundance data to inform the best timepoints to test for the *in vitro* experiments. All husbandry and sampling protocols for *A. fulvescens* followed the guidelines designated by the Canadian Council for Animal Care (#F15-007).

Table 1: *Acipenser fulvescens* intestinal tissue weights (mean ± SEM)

Tissue	One-year-old	Two-year-old
Anterior intestine	0.47 ± 0.03 g	2.44 ± 0.15 g
Spiral valve	0.64 ± 0.05 g	2.32 ± 0.15 g

2.1.2 *Squalus suckleyi:*

Twenty-one wild adult male North Pacific spiny dogfish (*Squalus suckleyi*; 2.1 ± 0.1 kg*)* were collected using baited hook and line from Barkley Sound, British Columbia. Collection permission was granted by the Department of Fisheries and Oceans Canada (XR-199 2022). After retrieval from the wild, they were held in continuously flowing seawater in a ~150 000 L tank at 12 ± 1°C. *S. suckleyi* were offered approximately 2% of the total mass of all *S. suckleyi* present in the tank of white fish and fed until satiation. Subsequently, they were given an abdominal massage to feel for food pieces in the stomach. Once evidence of feeding was obtained, *S. suckleyi* were moved into 5000 L tanks with continuously flowing seawater at 12 ± 1°C, where they were housed in until the post-feeding timepoints of 6 hours (6 h 28 min ± 15 min), 24 hours (25 h 15 min ± 16 min), or a minimum of 7 days (7+ days). All *S. suckleyi* husbandry and sampling protocols followed the guidelines designated by the Canadian Council

for Animal Care and were approved by the Bamfield Marine Sciences Centre's Animal Care Committee (RS-22-10).

2.2.0 Materials:

Millipore-Sigma (St. Louis, Missouri, USA) supplied all chemical compounds unless otherwise stated.

2.3.0 Tissue processing:

2.3.1 One-year-old *Acipenser fulvescens*:

At their designated post-feeding timepoints (6 hours, 24 hours, 96 hours, or 7+ days), one-year-old *A. fulvescens* were euthanized with an overdose of tricaine methanesulfonate (MS-222; 200 mg L^{-1}; Syndel Laboratory, Nanaimo, Canada) buffered with an equivalent amount of sodium bicarbonate. Once weighed, their gastrointestinal tracts were carefully excised and divided into the following sections: stomach, pyloric ceca, anterior intestine, anterior- and posterior spiral valve. Tissue sections were weighed then rinsed with *A. fulvescens* Ringer's solution (pH 7.6 in mM; 126, NaCl; 2.2, KCl; 0.45 mM, $CaCl_2 \cdot 2H_2O$; 3, $MgCl_2 \cdot 6H_2O$; 4.6, $Na_2HPO_4 \cdot 2H_2O$; 0.2, KH_2PO_4; based on Allen et al., 2009) to remove excess chyme and mucus. A portion of each gastrointestinal section was frozen in liquid nitrogen and stored at -80°C for enzymatic analysis. An additional portion intended for molecular experimentation was submerged in RNA*later*™ Stabilization Solution (Thermo Fisher Scientific, Waltham, USA), placed at 4°C overnight, then stored at -20°C.

2.3.2 Two-year-old *Acipenser fulvescens*:

Two-year-old *A. fulvescens* were euthanized as described in section 2.2.1 at their designated post-feeding timepoints (6 hours, 24 hours, or 7+ days), then weighed. Their anterior intestines and spiral valves were subsequently isolated and rinsed with lake sturgeon Ringer's solution (section 2.3.1). Each tissue region was weighed then allocated for *in vitro* experimentation.

2.3.3 *Squalus suckleyi:*

At the appropriate post-feeding timepoints (6 hours, 24 hours, or 7+ days), *S. suckleyi* were euthanized with an overdose of MS-222 (200 $mg \cdot L^{-1}$ in seawater; Syndel Laboratory) and then weighed. The gastrointestinal tract was removed, and the following regions were isolated: cardiac stomach, pyloric stomach, spiral valve, and colon. Each segment was rinsed to remove excess chyme and mucus with elasmobranch Ringer's solution (pH 7.4 in mM; 400, urea; 257, NaCl; 80, TMAO; 7, Na_2SO_4; 6, $NaHCO_3$; 4, KCl; 3, $MgSO_4 \cdot 7H_2O$; 2, $CaCl_2 \cdot 2H_2O$; 0.1, Na_2HPO_4), and then weighed. The spiral valve was then divided into anterior, mid, and posterior segments. Spiral valve tissues were first allocated towards the *in vitro* section of this study. Portions of all aforementioned gastrointestinal segments were also divided for enzymatic and molecular analysis and were further processed as described in section 2.3.1.

2.4.0 Maltase activity:

Maltase activity was measured indirectly by determining glucose production after adding maltose to the supernatant of epithelial scrapings (see Weinrauch et al., 2018) and glucose production was measured using an assay adapted from Treberg et al. (2007). Prior to determining maltase activity, gastrointestinal tissues were thawed in homogenization buffer (pH 7.4 in mM; 50, imidazole; 1, EDTA). The epithelial layer of each tissue segment was removed using a glass microscope slide. I analyzed pyloric ceca from *A. fulvescens* using whole tissue segments due to their morphology. For both *A. fulvescens* and *S. suckleyi,* I validated the use of epithelial scrapings by comparing their measurements to corresponding underlying tissue and whole tissue samples in the spiral valve regions (96 hours post-fed *A. fulvescens* and 6 hours post-fed *S. suckleyi*). Underlying scraped tissue samples were rinsed in homogenization buffer to remove residual epithelial tissue. Tissues were appropriately diluted and homogenized (VWR 4-Place Mini Bead Mill Homogenizer; Avantor, Randor, PA, USA) in homogenization buffer and subsequently centrifuged (15 000 x g at 4 °C) for 30 min.

In duplicate using clear, flat-bottomed 96-well microplates, 15 µL of homogenized supernatant was combined with either 15 µL of 60 mM maltose or deionized water (negative control). After a 20-min incubation, 200 µL of reaction buffer (pH 7.4 at room temperature in mM; 500, imidazole; 5, $MgSO_4$; 10, ATP; 0.8, $NADP^+$) and 1 $unit \cdot mL^{-1}$ glucose-6-phosphate dehydrogenase were added. After a subsequent 10-min incubation period, 1 $unit \cdot mL^{-1}$

hexokinase was added for a final assay volume of 250 µL. Absorbance was measured spectrophotometrically at 340 nm until constant with a microplate spectrophotometer (PowerWave XS2; Biotek, Winooski, VT, USA) using Gen5 software (Biotek). Glucose content was determined by comparing the change in absorbance to the corresponding negative control (to account for endogenous glucose) then transforming the resulting value to mmol·L^{-1} using a glucose standard curve. Maltase activity is represented as mM glucose·mg wet tissue mass·min^{-1}.

2.5.0 *sglt1* mRNA transcript abundance:

A glass microscope slide was used to remove the epithelial layer of each gastrointestinal tissue sample. Whole tissue was used for pyloric ceca samples from *A. fulvescens* due to their morphology. TRIzol Reagent (Thermo Fisher Scientific, Waltham, MA, USA) was used to isolate RNA from epithelial scrapings following the manufacturers protocol. Newly isolated RNA quality and quantity were examined for all samples using a NanoDrop 2000c (Thermo Fisher Scientific) followed by gel electrophoresis to assess RNA integrity. RNA samples were stored at −80°C prior to cDNA synthesis.

To remove any traces of DNA contamination, all RNA samples underwent a DNasing step using the Invitrogen™ DNase I Amplification Grade kit (Thermo Fisher Scientific). cDNA was then synthesized from 1 µg of DNase-treated RNA using the iScript™ cDNA Synthesis Kit (Bio-Rad Laboratories Inc, Hercules, CA, USA). After synthesis, cDNA samples were stored at −20°C. All kits were used following the manufacturer's instructions.

In preparation for real-time quantitative polymerase chain reaction (RT-qPCR), *A. fulvescens sglt1* RT-qPCR primers (Table 2) were designed based on an annotated gastrointestinal tract transcriptome from each of the glandular stomach, muscular stomach, anterior intestine, pyloric cecum, spiral valve, and rectum. These transcriptomes were assembled by Thorstensen et al. (2023). The *S. suckleyi sglt1* RT-qPCR primers used were previously designed and validated by Deck et al. (2017; Table 2). RT-qPCR was conducted in duplicate using per reaction 5 µL SsoAdvanced Universal SYBR Green Supermix (Bio-rad Laboratories Inc), 2.5 µL of 3.2 µM primers, 2.5 µL of cDNA template diluted in nuclease-free water to bring the total reaction mix to 10 µL. Cycling conditions for *A. fulvescens sglt1* were as follows: 95°C for 3 min followed by 35 cycles of a 2-step cycle of 15 s at 95°C, and 30 s at 60°C (106%

efficiency). For *S. suckleyi sglt1*: 95°C for 10 min followed by 39 cycles of a 2-step cycle of 10 s at 95°C, and 15 s at 60°C (106% efficiency). At the end of each cycling protocol, a melt curve analysis was performed.

I was unable to validate a stable endogenous control gene between different gastrointestinal tissues and different postprandial timepoints for both *A. fulvescens* and *S. suckleyi.* Thus, I designed gBlocks™ gene fragments (customizable double stranded DNA fragments) which included partial sequences from both *A. fulvescens* and *S. suckleyi sglt1,* synthesized by Integrated DNA Technologies (IDT, Coralville, IA; Table 2). A standard curve was constructed using the gBlocks™ gene fragments to determine the copy number of *sglt1* in corresponding *A. fulvescens* and *S. suckleyi* samples (Weinrauch et al., 2022a).

Table 2: Primer and gBlocks™ information for *Acipenser fulvescens* and *Squalus suckleyi sglt1* genes

Target	Sequence	Product length (base pairs)	Annealing temperature (°C)
A. fulvescens: sglt1 forward primer	5'-CAG CCA GTG CCC CAA GA-3'	74	60
A. fulvescens: sglt1 reverse primer	5'-TGC AGG AGA TGC CGA AGA-3'	74	60
S. suckleyi: sglt1 forward primer	5'-CAGAGCTGGAGTTGTGACCA-3'	157	60
S. suckleyi: sglt1 reverse primer	5'-CAGTGCCTCCCGGATAAATA-3'	157	60
A. fulvescens and *S. suckleyi: sglt1* gBlocks™	5’-GATGGCTGTTTGTACCGATCTACATCAG AGCTGGAGTTGTGACCATGCCTGAGTACC TGAAGAGGCGATTCGGGGGCAATCGGATC AGGATTTACCTGTCTGTCCTCTCGCTGTGC CTCTACATATTCACCAAGATATCGGCTGAC ATGTTTTCAGGAGCCATATTTATCCGGGAG GCACTGGGATTGAACCTGTACGTTGCCGT GGATGGCACCGGCAGCTGTGTGACCCCCA GCCAGTGCCCCAAGATCATCTGCGGCGTC CACTACCTCTACTTCGCACTCATTCTCTTCG GCATCTCCTGCATCATCATCCTGGGGGTGT CCCTGAT-3’	N/A	N/A

2.6.0 *in vitro* intestinal fluxes:

2.6.1 *Acipenser fulvescens:*

Intestinal tissues (spiral valve and anterior intestine) were mounted using tissue holders with a 0.3 cm^2 aperture (P2310; Physiologic Instruments, Reno, NV USA) and placed in Ussing chambers (EM-CSYS-2; Physiologic Instruments). After chamber assembly, 4 mL of either 0.25, 0.5, 2.5, 5, or 10 mM glucose *A. fulvescens* Ringer's with radiolabelled ^{14}C-glucose (0.01 $\mu Ci \cdot mL^{-1}$; PerkinElmer, USA) were added to the mucosal side of each chamber. 4 mL of appropriate Ringer's solution without the addition of ^{14}C-glucose was added to the serosal side of each chamber. The serosal solution was osmotically balanced to the mucosal solution using mannitol and osmotic pressure was verified using an osmometer (VAPRO Vapor Pressure Osmometer Model 5520; Wescor, Logan, UT). The tissue preparations were incubated for 3 hours while being supplied with a specialty gas mix (99.7% O_2: 0.3% CO_2) and chilled to 16 ± 1°C using a recirculating chiller. Initial and final samples from the mucosal and serosal chambers were taken; their radioactivity was counted in duplicate on a liquid scintillation counter (Tri-Carb 3110 TR; PerkinElmer) by combining 200 µL of sample with 3.5 mL scintillation cocktail (OptiPhase HiSafe 3, PerkinElmer). No final serosal samples had counts over twice the background, indicating that leakage did not occur.

2.6.2 *A. fulvescens* sodium and SGLT1 dependent *in vitro* intestinal fluxes:

I conducted a set of *in vitro* fluxes in 24 hours post-fed *A. fulvescens* using the SGLT1 inhibitor phlorizin (Raja & Kinne, 2015) and with low sodium Ringer's to determine the impact of both SGLT1 inhibition and sodium dependence on glucose uptake. After mounting intestinal tissues following the protocol in section 2.6.1, the tissues incubated in low sodium *A. fulvescens* Ringer's solution for a minimum of 20 minutes (pH 7.6 in mM; 126, $[(CH_3)_3NCH_2CH_2OH]^+Cl^-$; 2.2, KCl; 0.45 mM, $CaCl_2 \cdot 2H_2O$; 3, $MgCl_2 \cdot 6H_2O$; 4.6, $Na_2HPO_4 \cdot 2H_2O$) to help reduce endogenous sodium. Mucosal chambers were then filled with 4 mL of ^{14}C-glucose (0.01 $\mu Ci \cdot mL^{-1}$) in either: 5 mM glucose Ringer's, 5 mM glucose Ringer's with 0.25 µM phlorizin, 5 mM glucose Ringer's with 10 µL DMSO (equivalent to the volume of phlorizin added in the phlorizin treatment; vehicle control), or 5 mM glucose low sodium Ringer's. Phlorizin was initially reconstituted in DMSO. The serosal chambers were filled with 4 mL of either low

sodium or regular osmotically balanced Ringer's solution. The preparations then fluxed as described in section 2.6.1.

2.6.3 *Squalus suckleyi:*

Modified Ussing-like chambers were used based on Anderson et al. (2015) over traditional Ussing chambers (section 2.5.1) to increase the fluxing surface area. Spiral valve folds were placed over the openings of 7 mL scintillation vials and lids with a 1.13 cm^2 aperture fastened the tissues in place (Figure 4). Sides of the tissues facing the inside of the scintillation vials were designated as the mucosal side. 2 mL of either 0.25, 1, 0.5, 2.5, 5, or 10 mM glucose elasmobranch Ringer's solution plus ^{14}C-glucose (0.02 μCi·mL^{-1}; PerkinElmer) was added to the mucosal side of the chamber. Additionally, 2 mL of 5 mM glucose low sodium elasmobranch Ringer's solution (pH 7.4 in mM; 400, urea; 257, N-methyl-d-glucamine; 80, TMAO; 7, Na_2SO_4; 6, $NaHCO_3$; 4, KCl; 3, $MgSO_4 \cdot 7H_2O$; 2, $CaCl_2 \cdot 2H_2O$; 0.1, Na_2HPO_4) was used when testing sodium-dependent glucose uptake. I did not use phlorizin as described in section 2.6.2 because it did not make it out to our field station. Mucosal solutions were pre-equilibrated with specialty gas mixture (99.7% O_2: 0.3% CO_2) to ensure sufficient oxygenation prior to addition to the chamber. In advance of the tissue incubation, initial mucosal and serosal solution samples were taken. Each chamber was weighed to 1 mg accuracy, prior to inversion into 50 mL falcon tubes (serosal chamber) containing 5 mL of elasmobranch Ringer's solutions osmotically balanced with mannitol (VAPRO Vapor Pressure Osmometer Model 5520; Wescor). The Ussing-like chamber preparations were then incubated in a bath of flow-through seawater maintained at 12 ± 1°C for 3 hours. Post incubation, the preparations were blotted dry, reweighed, and mucosal and serosal fluid samples were taken. The radioactivity of samples was counted in duplicate on a liquid scintillation analyzer (Tri-Carb 3110 TR; PerkinElmer) by combining 100 μL of sample with 4 mL scintillation cocktail (Ultima Gold XR; PerkinElmer). The final preparations did not exhibit weight differences over 50 mg and final serosal samples did not have counts over twice the background, indicating that leakage did not occur in any preparations.

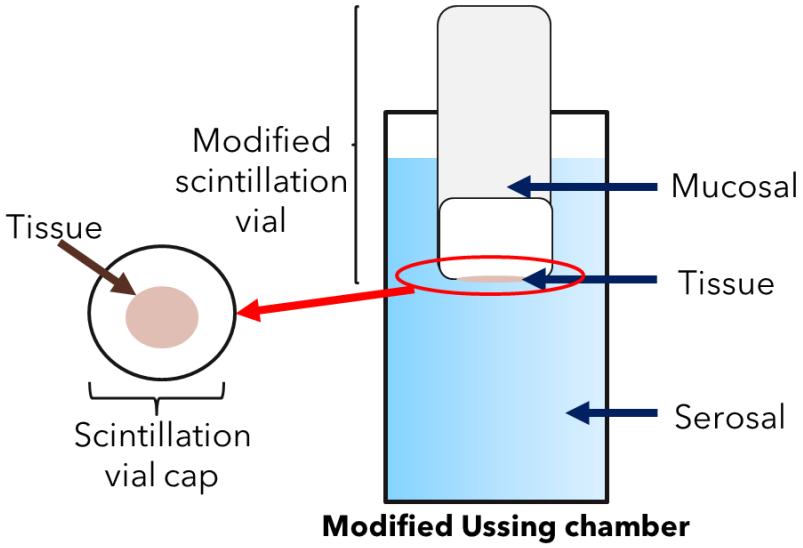

Figure 4*:* Diagram depicting the setup for the modified Ussing chambers used for *Squalus suckleyi.* Note that an air line was delivering oxygen into the serosal chamber but was not included in the diagram for clarity.

2.6.4 Tissue digestions:

Tissues were rinsed in a corresponding supersaturated glucose Ringer's solution post incubation to remove adsorbent ^{14}C-glucose radiolabel (tissues from section 2.6.2 used low sodium Ringer's). Subsequently, they were digested in 1 N nitric acid at 60°C. Digested tissues (1 mL *A. fulvescens;* 100 µL *S. suckleyi*) were combined with scintillation fluid (3.5 mL *A. fulvescens;* 4 mL *S. suckleyi*; Ultima Gold XR; PerkinElmer) and counted using a liquid scintillation analyzer (Tri-Carb 3110 TR; PerkinElmer). *S. suckleyi* tissue digests were run in duplicate; *A. fulvescens* samples did not have enough tissue to run in duplicate. Manual quench correction was used for tissue digests by generating species specific quench curves over a range of tissue masses.

2.6.5 Calculations:

Glucose is typically converted into glucose-6-phosphate after crossing the luminal cell membrane to maintain the concentration gradient of glucose absorption (Cox, 2013), making

serosal appearance of the label not fully representative of glucose uptake. Unidirectional uptake was ascertained by measuring disappearance of ^{14}C-glucose from the experimental (mucosal) solution (J_{ms}) in μmol glucose·cm^{-2}·h^{-1} using the following equation:

$$J_{ms} = \frac{(C_i \cdot V_i) - (C_f \cdot V_f)}{A \cdot T}$$

Where A represents surface area (cm^2), and T represents flux time (h). C and V represent the concentration of glucose (μmol) and volume (mL) of the mucosal solution at the beginning (i) and end (f) of the flux. Since the glucose was radiolabeled, C_i and C_f were calculated in advance utilizing:

$$C = \frac{R}{V_s \cdot SA}$$

Where R represents radioactivity (CPM), V_s represents the volume of sample (mL), and SA represents specific activity (CPM·μmol^{-1}). Tissue uptake (μmol·g·h^{-1}) was calculated using:

$$Uptake = \frac{C \cdot V_t}{m \cdot T}$$

In which the C and T are the same as above (note that CPM values are quench corrected), m represents wet tissue mass (g) and V_t represents the volume of digested tissue sample.

2.7.0 Data Analysis:

Concentration dependent kinetic curves were generated and analyzed using GraphPad Prism (ver. 8.0.2; GraphPad Software INC., La Jolla, CA, USA). Individual data were fitted to linear and hyperbolic curves using least squares regression (additionally forcing curves to start at x=0, y=0) and compared using the extra sum-of-squares *F* test to determine the best-fitting model (null hypothesis=linear model, alternative hypothesis=hyperbolic model). Comparisons where I could not reject the null hypothesis, the data were fit to the curve that produced the highest R^2 value for graphing purposes. Michaelis-Menten kinetics (K_m and V_{max}) were calculated by GraphPad Prism for data that best fit hyperbolic curves. Differences in *sglt1* mRNA transcript abundance and maltase activity at different postprandial timepoints within each

tissue region were analyzed via 1-way analysis of variance (ANOVA) with normality and homogeneity of variance assumptions met with Shapiro–Wilk and Levene's tests. Datasets with non-normal distribution or heterogeneous variances were transformed using log, inverse, or square root transformations depending on the data distribution. Datasets that did not meet these assumptions after being transformed were analyzed using Kruskal-Wallis non-parametric tests. Tukey's and Dunn's multiple comparisons post hoc tests were used when appropriate for 1-way ANOVAs and Kruskal-Wallis tests. Data were considered significantly different at an α level of 0.05 for all tests. All data were visualized and analyzed using GraphPad Prism (ver 8.0.2), except for Levene's tests, which were generated using Microsoft Excel (Version 2304).

3.0.0 Results:

3.1.0 Maltase activity:

The spiral valve epithelial layer had significantly higher maltase activity than the underlying tissue of *A. fulvescens* (Figure 5A and Table 3; anterior spiral valve: p<0.0001****; posterior spiral valve: p<0.0001****, $F_{2,17}$=37.44). A similar trend was found in the anterior spiral valve region of *S. suckleyi* (Figure 5B and Table 3; p=0.0165*, $F_{2,16}$=5.361). However, there was no difference between the epithelial scrapings and underlying tissue maltase activity in the mid and posterior spiral valve (Figure 5B and Table 3).

A significant increase in maltase activity 7+ days post-feeding was evident in the stomach regions of *A. fulvescens* (Figure 6A and Table 4; p=0.0403*, $F_{3,21}$=3.301) and *S. suckleyi* (pyloric stomach only; Figure 6B and Table 4; p=0.001**, $F_{2,15}$=11.22). Following the stomach, an anterior to posterior wave of maltase activity was evident in *A. fulvescens;* there was a significant decrease in activity in the pyloric ceca 96 hours post-feeding (Figure 6A and Table 4; p<0.0001****, $F_{3,23}$=18.42), a decrease in the anterior intestine 7+ days post-feeding (Figure 6A and Table 4; p=0.007**, H_1=12.11), and an increase in the posterior spiral valve 96 hours post-feeding (Figure 6A and Table 4; p=0.014*, $F_{3,21}$=4.446). A similar wave of activity was present in the spiral valve of *S. suckleyi* with a significant increase and subsequent decrease at 24 hours in the anterior spiral valve (Figure 6B and Table 4; p=0.0047**, $F_{2,17}$=7.479), and a prolonged increase at 24 hours in the mid spiral valve (Figure 6B and Table 4; p=0.0008***, $F_{2,15}$=11.82). There was no impact of feeding on maltase activity in the anterior spiral valve in

A. fulvescens, and the cardiac stomach, posterior spiral valve, and colon in *S. suckleyi* (Figure 6 and Table 4).

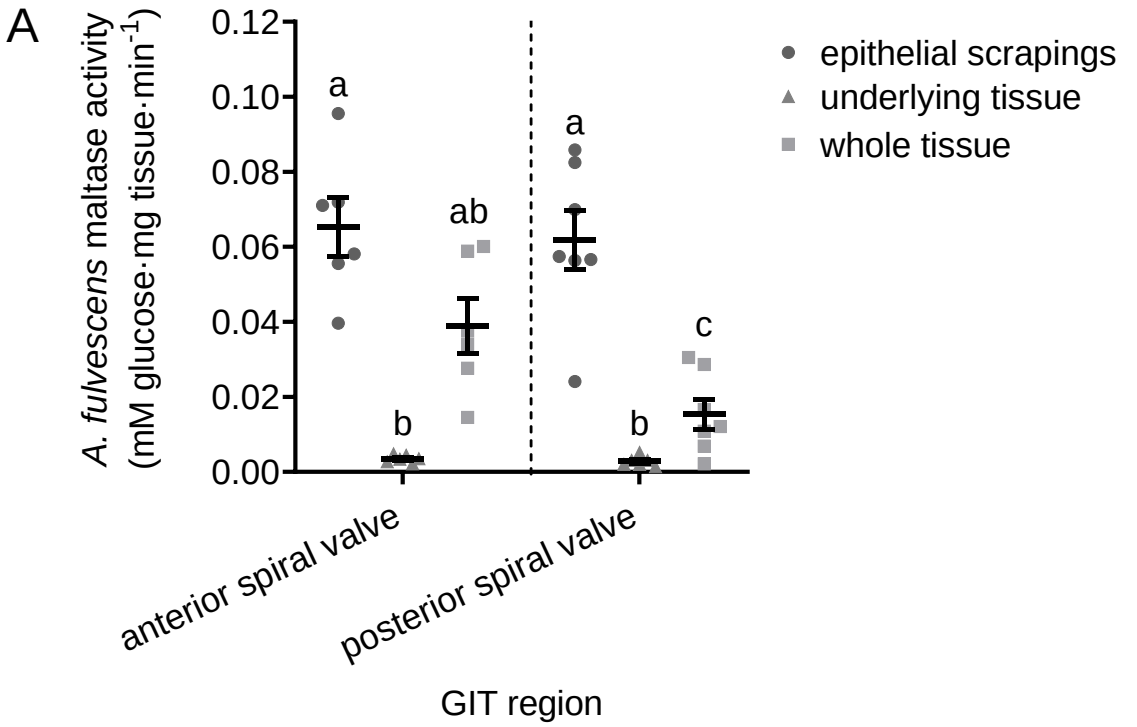
A
A. fulvescens maltase activity
(mM glucose·mg tissue·min-1)
0.12
0.10
0.08
0.06
0.04
0.02
0.00
a
b
ab
a
b
c
epithelial scrapings
underlying tissue
whole tissue
anterior spiral valve
posterior spiral valve
GIT region

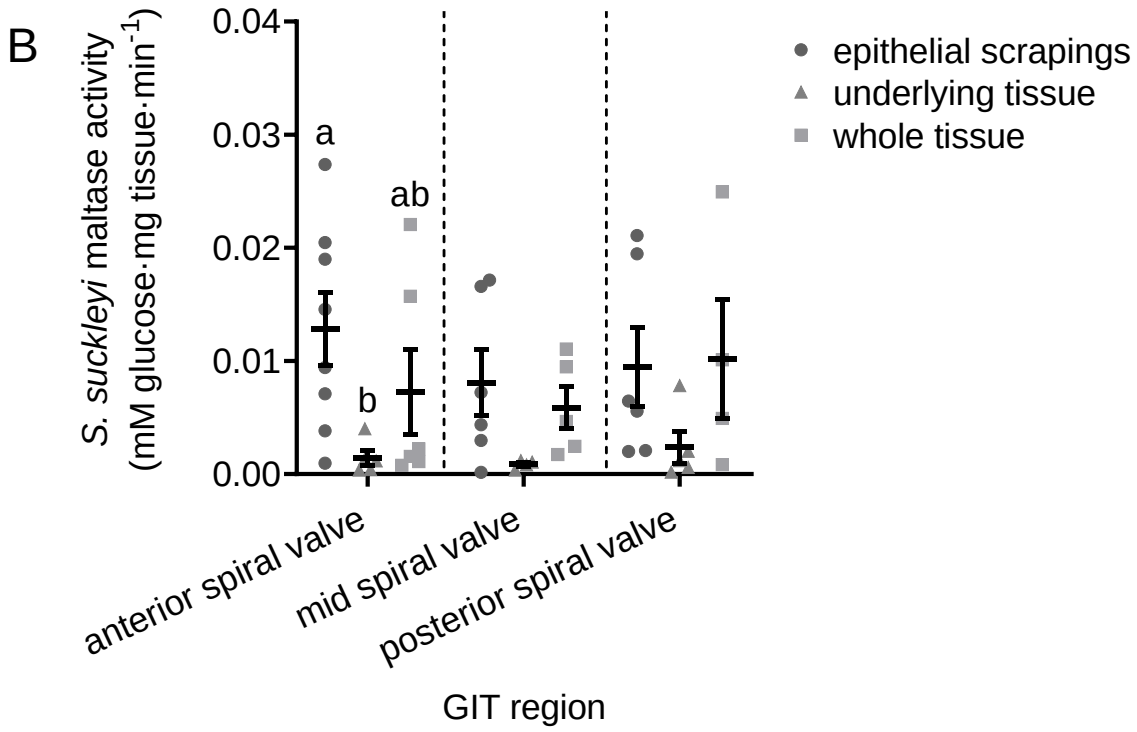
B
S. suckleyi maltase activity
(mM glucose·mg tissue·min-1)
0.04
0.03
0.02
0.01
0.00
a
b
ab
epithelial scrapings
underlying tissue
whole tissue
anterior spiral valve
mid spiral valve
posterior spiral valve
GIT region

Figure 5: Indirect measurement of maltase activity (mM glucose·mg wet tissue mass·min^{-1}) through glucose production from maltose in different tissue layers in the spiral valve of *Acipenser fulvescens* (A; n=6-7; 96 hours post-fed) and *Squalus suckleyi* (B; n=4-8; 6 hours post-fed). Measurements were taken either in epithelial scrapings (circles), underlying tissue (triangles), or whole tissue (squares) and are presented as means ± SEM. 1-way ANOVAs were conducted in each gastrointestinal region with corresponding Tukey's post hoc tests, except for the anterior spiral valve in *A. fulvescens* which was analyzed using a Kruskal-Wallis test with a Dunn's post hoc test. Dotted lines signify separation in statistical tests and significant differences (α=0.05) are indicated by lowercase letters.

Table 3: Summary of statistics analyzing the impact of spiral valve tissue layers on *Acipenser fulvescens* and *Squalus suckleyi* maltase activity.

Species	GIT Region	Transformation Used	Statistical Test	*F*	Degrees of Freedom (DFn, DFd)	*p*	R^2	Kruskal-Wallis statistic (*H*)
A. fulvescens	anterior spiral valve	N/A	Kruskal-Wallis	N/A	N/A	<0.0001****	N/A	13.05
A. fulvescens	posterior spiral valve	log	1-way ANOVA	37.44	2, 17	<0.0001****	0.815	N/A
S. suckleyi	anterior spiral valve	log	1-way ANOVA	5.361	2, 16	0.0165*	0.4013	N/A
S. suckleyi	mid spiral valve	log	1-way ANOVA	2.753	2, 12	0.1037	0.3146	N/A
S. suckleyi	posterior spiral valve	log	1-way ANOVA	2.833	2, 12	0.0983	0.3207	N/A

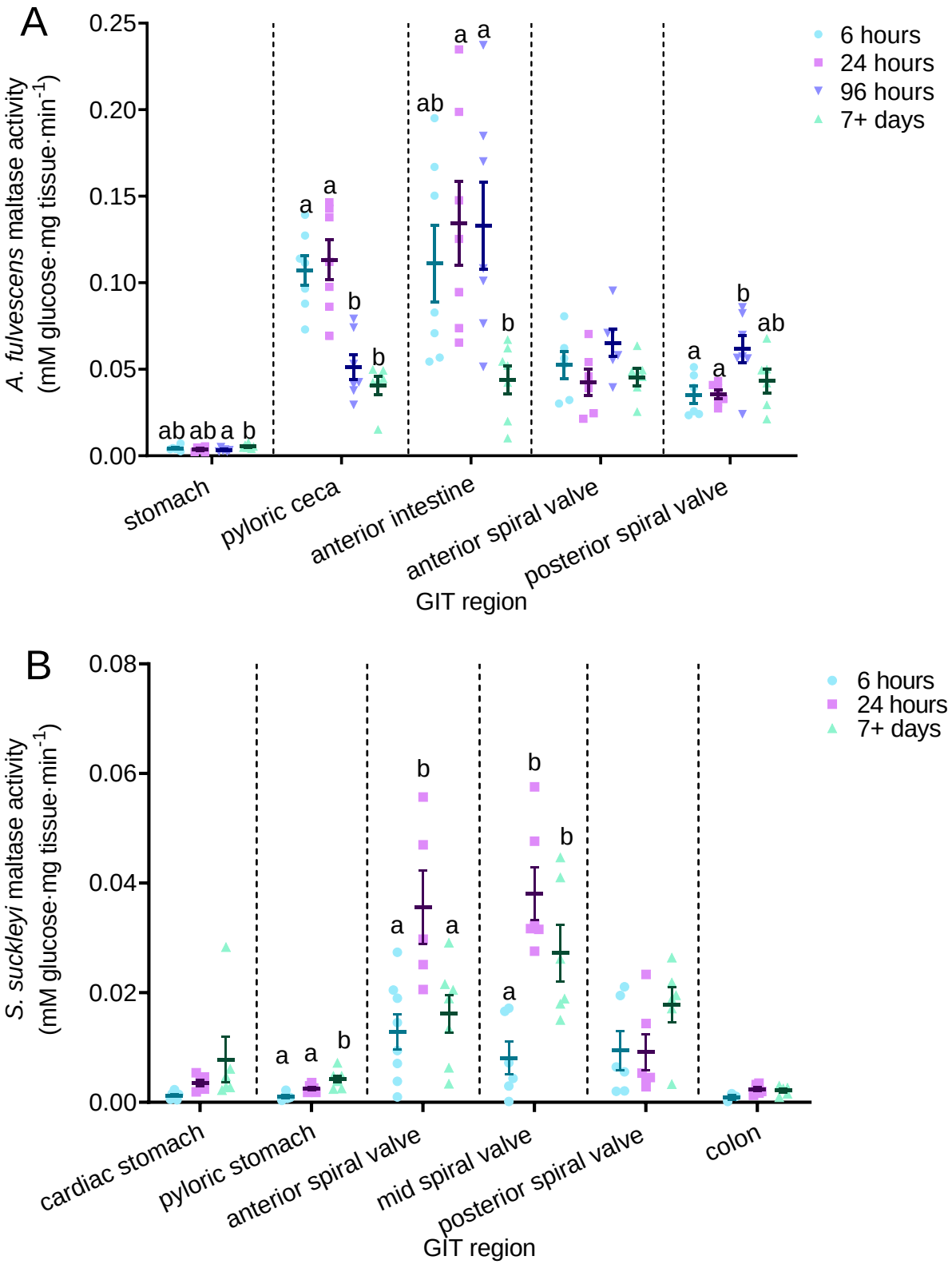
A
A. fulvescens maltase activity
(mM glucose·mg tissue·min-1)
0.25
0.20
0.15
0.10
0.05
0.00
ab ab a b
a a b b
ab a a b
a a b ab
6 hours
24 hours
96 hours
7+ days
stomach
pyloric ceca
anterior intestine
anterior spiral valve
posterior spiral valve
GIT region
B
S. suckleyi maltase activity
(mM glucose·mg tissue·min-1)
0.08
0.06
0.04
0.02
0.00
a a b
a a
a b b
b
6 hours
24 hours
7+ days
cardiac stomach
pyloric stomach
anterior spiral valve
mid spiral valve
posterior spiral valve
colon
GIT region

Figure 6: Indirect measurement of maltase activity (mM glucose·mg wet tissue mass·min^{-1}) through glucose production from maltose at different postprandial timepoints along the gastrointestinal tract (GIT) of *Acipenser fulvescens* (A; n=6-7) and *Squalus suckleyi* (B; n=3-8). Data are presented as means ± SEM. Measurements were taken either 6 hours (circles), 24 hours (squares), 96 hours (downward triangles; only A. fulvescens), or 7+ days (upright triangles) after feeding. Dotted lines signify separation in statistical tests. 1-way ANOVAs were conducted in each gastrointestinal region with corresponding Tukey's post hoc tests. Exceptions include the anterior intestine (*A. fulvescens*) and posterior spiral valve (*S. suckleyi*) which were analyzed using Kruskal-Wallis tests with Dunn's post hoc tests. Significant differences (α=0.05) are indicated by lowercase letters.

Table 4: Summary of statistics analyzing the impact of a postprandial timeseries on maltase activity in various gastrointestinal tissues in *Acipenser fulvescens* and *Squalus suckleyi*.

Species	GIT Region	Transformation Used	Statistical Test	*F*	Degrees of Freedom (DFn, DFd)	*p*	R^2	Kruskal-Wallis statistic (*H*)
A. fulvescens	stomach	N/A	1-way ANOVA	3.301	3, 21	0.0403*	0.3205	N/A
A. fulvescens	pyloric ceca	N/A	1-way ANOVA	18.42	3, 23	<0.0001****	0.7061	N/A
A. fulvescens	anterior intestine	N/A	Kruskal-Wallis	N/A	N/A	0.007**	N/A	12.11
A. fulvescens	anterior spiral valve	N/A	1-way ANOVA	2.022	3, 20	0.1431	0.2328	N/A
A. fulvescens	posterior spiral valve	N/A	1-way ANOVA	4.446	3, 21	0.0144*	0.3884	N/A
S. suckleyi	cardiac stomach	log	1-way ANOVA	0.7984	2, 16	0.4672	0.09074	N/A
S. suckleyi	pyloric stomach	N/A	1-way ANOVA	11.22	2, 15	0.001**	0.5994	N/A
S. suckleyi	anterior spiral valve	N/A	1-way ANOVA	7.479	2,17	0.0047**	0.468	N/A
S. suckleyi	mid spiral valve	N/A	1-way ANOVA	11.82	2, 15	0.0008***	0.6119	N/A
S. suckleyi	posterior spiral valve	N/A	Kruskal-Wallis	N/A	N/A	0.2551	N/A	2.842
S. suckleyi	colon	N/A	1-way ANOVA	3.279	2, 12	0.0731	0.3534	N/A

3.2.0 *sglt1* mRNA transcript abundance:

At the 24 hours and 7+ days post-feeding timepoints, RNA of sufficient quantity and quality wasn't successfully isolated from the stomach regions and colon of *S. suckleyi*. Therefore, these regions were not included in the postprandial timeseries analysis (Figure 8B and Table 6). However, *sglt1* mRNA transcript abundance from all regions of the gastrointestinal tract was determined at 6 hours post-feeding (Figure 7). The spiral valve regions had significantly higher *sglt1* transcript abundance than the other gastrointestinal regions (Figure 7 and Table 5; p<0.0001****, $F_{5,34}$=14.36).

In *A. fulvescens*, there were no gastrointestinal regions that exhibited significant postprandial changes in *sglt1* mRNA abundance (Figure 8A and Table 6). In contrast, there was a significant increase in *sglt1* mRNA abundance in the mid spiral valve of *S. suckleyi* 24 hours post-feeding (Figure 8B and Table 6; p=0.0185*, $F_{2,15=5.265}$) with a fold change ~3 times higher than the abundance observed 6 hours post-feeding. This increase was also seen in maltase activity in the mid spiral valve at the same timepoint (section 3.1.0; Figure 6A and Table 4).

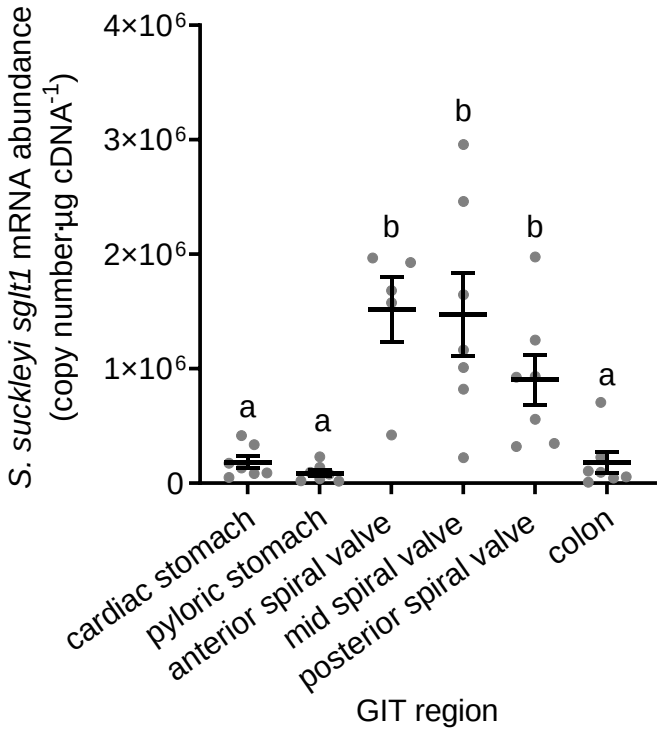

Figure 7: *Squalus suckleyi* (n=5-7) *sglt1* mRNA abundance (copy number·µg cDNA^{-1}) along the gastrointestinal tract 6 hours post-feeding. *Sglt1* copy numbers were determined through a standard curve created using gBlocks™ gene fragments which included a partial *sglt1* sequence from *S. suckleyi*. Data are presented as means ± SEM. A 1-way ANOVA with a corresponding Tukey's post hoc test was conducted, and statistical significance (α=0.05) is represented by lowercase letters.

Table 5: Summary of statistics analyzing the difference in *sglt1* mRNA abundance along the gastrointestinal tract of *Squalus suckleyi.*

Transformation Used	Statistical Test	*F*	Degrees of Freedom (DFn, DFd)	*p*	R^2
log	1-way ANOVA	14.36	5, 34	<0.0001****	0.6786

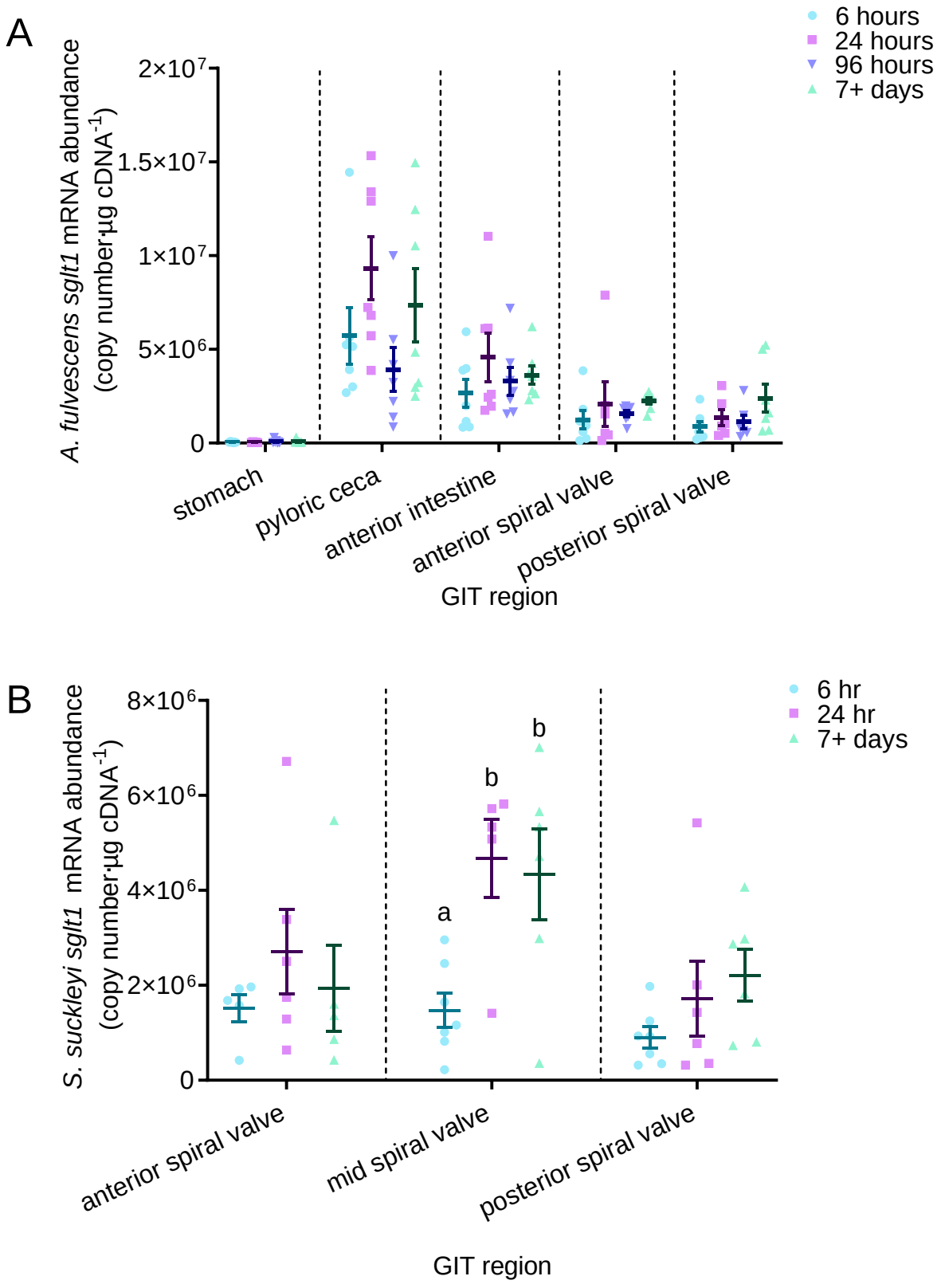
A
6 hours
24 hours
96 hours
7+ days
A. fulvescens sglt1 mRNA abundance
(copy number·µg cDNA-1)
2×10^7
1.5×10^7
1×10^7
5×10^6
0
stomach
pyloric ceca
anterior intestine
anterior spiral valve
posterior spiral valve
GIT region
B
6 hr
24 hr
7+ days
S. suckleyi sglt1 mRNA abundance
(copy number·µg cDNA-1)
8×10^6
6×10^6
4×10^6
2×10^6
0
a
b
b
anterior spiral valve
mid spiral valve
posterior spiral valve
GIT region

Figure 8: Impact of a postprandial timeseries on *sglt1* mRNA abundance (copy number·µg cDNA-1) along the gastrointestinal tract (GIT) of *Acipenser fulvescens* (A; n=6-7) and *Squalus suckleyi* (B; n=5-7). To determine the copy number of *sglt1* in gastrointestinal tissues, a standard curve was created using gBlocks™ gene fragments which included partial *sglt1* sequences from both organisms. Data are presented as means ± SEM at these postprandial timepoints: 6 hours (circles), 24 hours (squares), 96 hours (downward triangles; only *A. fulvescens*), and 7+ days (upright triangles). 1-way ANOVAs were conducted in each gastrointestinal region with corresponding Tukey's post hoc tests, excluding the anterior spiral valve in *A. fulvescens* which was analyzed using a Kruskal-Wallis test with a Dunn's post hoc test. Separation in statistical tests is indicated by dotted lines and statistical significance (α=0.05) is represented by lowercase letters.

Table 6: Summary of statistics analyzing the impact of a postprandial timeseries on *sglt1* mRNA abundance in various gastrointestinal tissues in *Acipenser fulvescens* and *Squalus suckleyi.*

Species	GIT Region	Transformation Used	Statistical Test	*F*	Degrees of Freedom (DFn, DFd)	*p*	R^2	Kruskal-Wallis statistic (*H*)
A. fulvescens	stomach	log	1-way ANOVA	0.4839	3, 22	0.6969	0.06191	N/A
A. fulvescens	pyloric ceca	log	1-way ANOVA	2.851	3, 24	0.0586	0.2627	N/A
A. fulvescens	anterior intestine	square root	1-way ANOVA	0.9361	3, 24	0.4386	0.1048	N/A
A. fulvescens	anterior spiral valve	N/A	Kruskal-Wallis	N/A	N/A	0.0691	N/A	7.089
A. fulvescens	posterior spiral valve	log	1-way ANOVA	1.918	3, 22	0.1562	0.2073	N/A
S. suckleyi	cardiac stomach	N/A	N/A	N/A	N/A	N/A	N/A	N/A
S. suckleyi	pyloric stomach	N/A	N/A	N/A	N/A	N/A	N/A	N/A
S. suckleyi	anterior spiral valve	square root	1-way ANOVA	0.6068	2, 13	0.5598	0.08538	N/A
S. suckleyi	mid spiral valve	square root	1-way ANOVA	5.265	2, 15	0.0185*	0.4124	N/A
S. suckleyi	posterior spiral valve	square root	1-way ANOVA	1.779	2, 16	0.2006	0.1819	N/A
S. suckleyi	colon	N/A	N/A	N/A	N/A	N/A	N/A	N/A

3.3.0 *in vitro* intestinal fluxes:

The concentration dependent glucose disappearance rates in the spiral valve and anterior intestine of *A. fulvescens* best fit a linear model due to their ambiguous fit of the hyperbolic model (Figure 9A-B and Table 7). The exception in both tissues was at the 24 hour timepoint, since I was unable to reject the null hypothesis that there was no difference between the two models (Table 7; anterior intestine: p=0.4876, $F_{1,27}$=0.4767; spiral valve: p=0.4963, $F_{1,25}$=0.4767). In the spiral valve of *S. suckleyi* at 7+ days the hyperbolic model fit the data best (Figure 9C and Table 5; p=0.0244, $F_{1,28}$=5.664, R^2=0.8649). At the other timepoints there was no difference between the fit of the two models (Table 7; 6 hours: p=0.0766, $F_{1,25}$=3.412; 24 hours: p=0.6497, $F_{1,31}$=0.2104). In contrast, for concentration dependent tissue glucose uptake in the spiral valve of *S. suckleyi* the hyperbolic model fit best for both 24 hours and 7+ days post-feeding (Figure 10 and Table 8; 24 hours: p=0.0094, $F_{1,34}$=7.574, R^2=0.6774; 7+ days: p=0.0048, $F_{1,40}$=8.936, R^2=0.72).

I calculated the Michaelis-Menten kinetics (K_m and V_{max}) for glucose dependent kinetic curves which best fit hyperbolic curves for both glucose disappearance rates (Figure 9) and tissue glucose uptake rates (Figure 10). For data calculated using glucose disappearance rates (Figure 9), I could only calculate K_m and V_{max} for the spiral valve in 7+ days post-fed *S. suckleyi* (Table 9). At the same timepoint and in the same fish, curves calculated using tissue uptake rates had both lower K_m and Vmax (Table 9; glucose disappearance: K_m=17.52, V_{max}=1.112; tissue uptake: K_m=8.188, V_{max}=0.02298). Using the same metric, both K_m and V_{max} were higher in 7+ days post-fed *A. fulvescens* in comparison to *S. suckleyi.* During the postprandial timeseries in the spiral valve of *S. suckleyi,* I determined that from 24 hours post-fed to 7+ days post-fed there was a decrease in V_{max} and an increase in K_m (Figure 10C and Table 9). The data for *A. fulvescens* overall fit linear models better than hyperbolic models. Therefore, I was unable to determine any changes in Michaelis-Menten parameters in *A. fulvescens* during different postprandial timepoints nor between the different intestinal regions (Table 9).

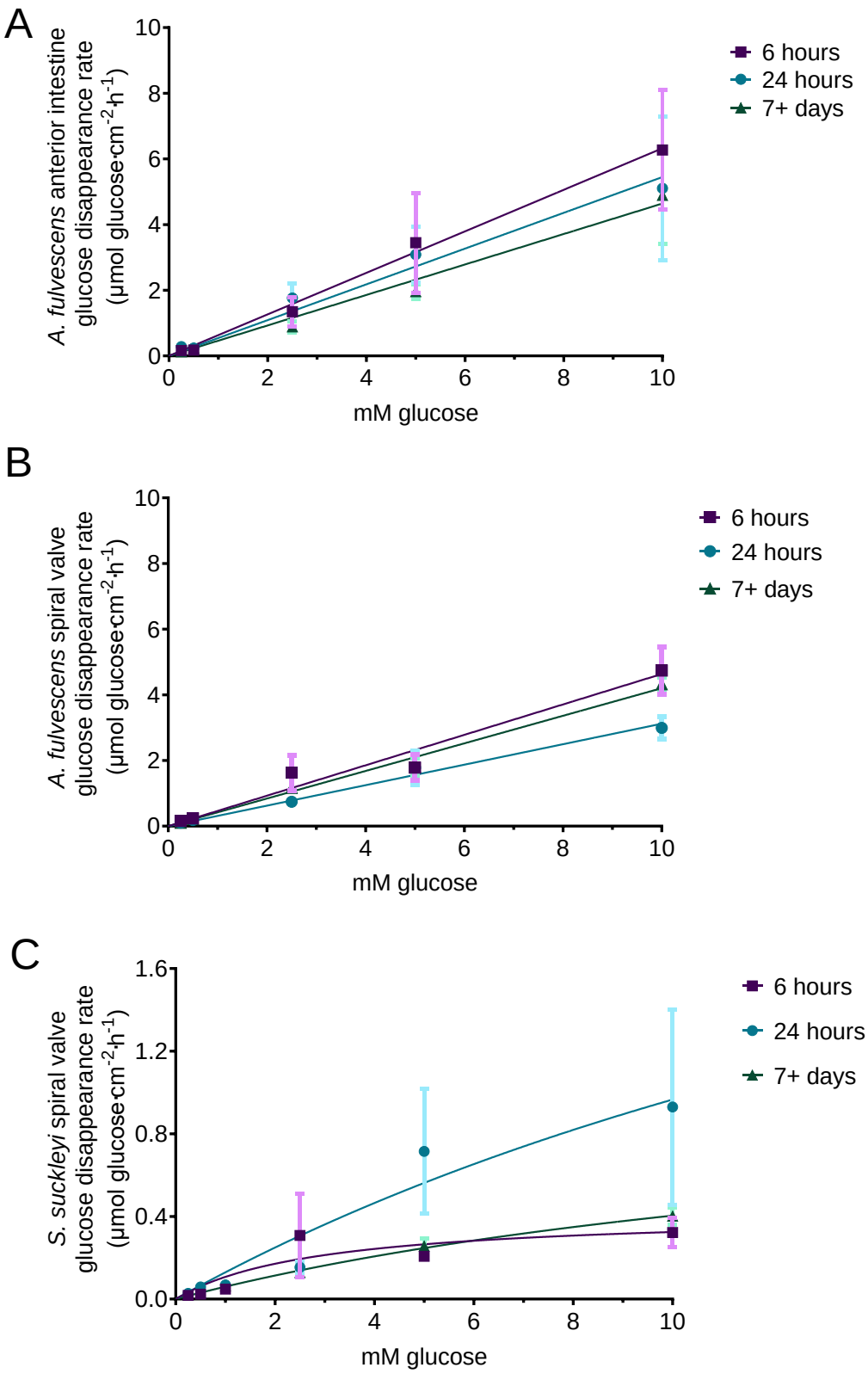
A
A. fulvescens anterior intestine
glucose disappearance rate
(µmol glucose·cm-2·h-1)
10
8
6
4
2
0
0
2
4
6
8
10
mM glucose
6 hours
24 hours
7+ days
B
A. fulvescens spiral valve
glucose disappearance rate
(µmol glucose·cm-2·h-1)
10
8
6
4
2
0
0
2
4
6
8
10
mM glucose
6 hours
24 hours
7+ days
C
S. suckleyi spiral valve
glucose disappearance rate
(µmol glucose·cm-2·h-1)
1.6
1.2
0.8
0.4
0.0
0
2
4
6
8
10
mM glucose
6 hours
24 hours
7+ days

Figure 9: Glucose dependent kinetic curves for the intestinal tissues of *Acipenser fulvescens* (anterior intestine: A, n=5-6; spiral valve: B, n=4-6) and *Squalus suckleyi* (spiral valve: C, n=3-6) during a postprandial time course. Glucose disappearance rate (μmol glucose $\cdot cm^{-2} \cdot h^{-1}$) data was collected with Ussing chambers for *A. fulvescens* and modified Ussing-like chambers for *S. suckleyi*; they are represented as means ± SEM at these post-feeding timepoints: 6 hours (pink squares), 24 hours (blue circles), and 7+ days (green triangles). Curves were fitted to either linear or hyperbolic models.

Table 7: Statistical summary table of linear and hyperbolic regressions of concentration dependent *in vitro* intestinal glucose disappearance (μmol glucose$\cdot cm^2 \cdot h^{-1}$) and corresponding sum-of-squares *F* tests (null hypothesis=linear model, alternative hypothesis=hyperbolic model) during different post-feeding timepoints in *Acipenser fulvescens* and *Squalus suckleyi*.

Species	Time post-fed	GIT Region	*F*	Degrees of Freedom (Den, Ded)	*p*	Linear R^2	Hyperbolic R^2
A. fulvescens	6 hours	anterior intestine	N/A	N/A	N/A	0.5109	ambiguous fit
A. fulvescens	24 hours	anterior intestine	0.4953	1, 27	0.4876	0.412	0.4226
A. fulvescens	7+ days	anterior intestine	N/A	N/A	N/A	0.5707	ambiguous fit
A. fulvescens	6 hours	spiral valve	N/A	N/A	N/A	0.7209	ambiguous fit
A. fulvescens	24 hours	spiral valve	0.4767	1, 25	0.4963	0.7778	0.782
A. fulvescens	7+ days	spiral valve	N/A	N/A	N/A	0.9309	ambiguous fit
S. suckleyi	6 hours	spiral valve	3.412	1, 25	0.0766	0.1612	0.2619
S. suckleyi	24 hours	spiral valve	0.2104	1, 31	0.6497	0.2918	0.2966
S. suckleyi	7+ days	spiral valve	5.664	1, 28	0.0244	0.8376	0.8649

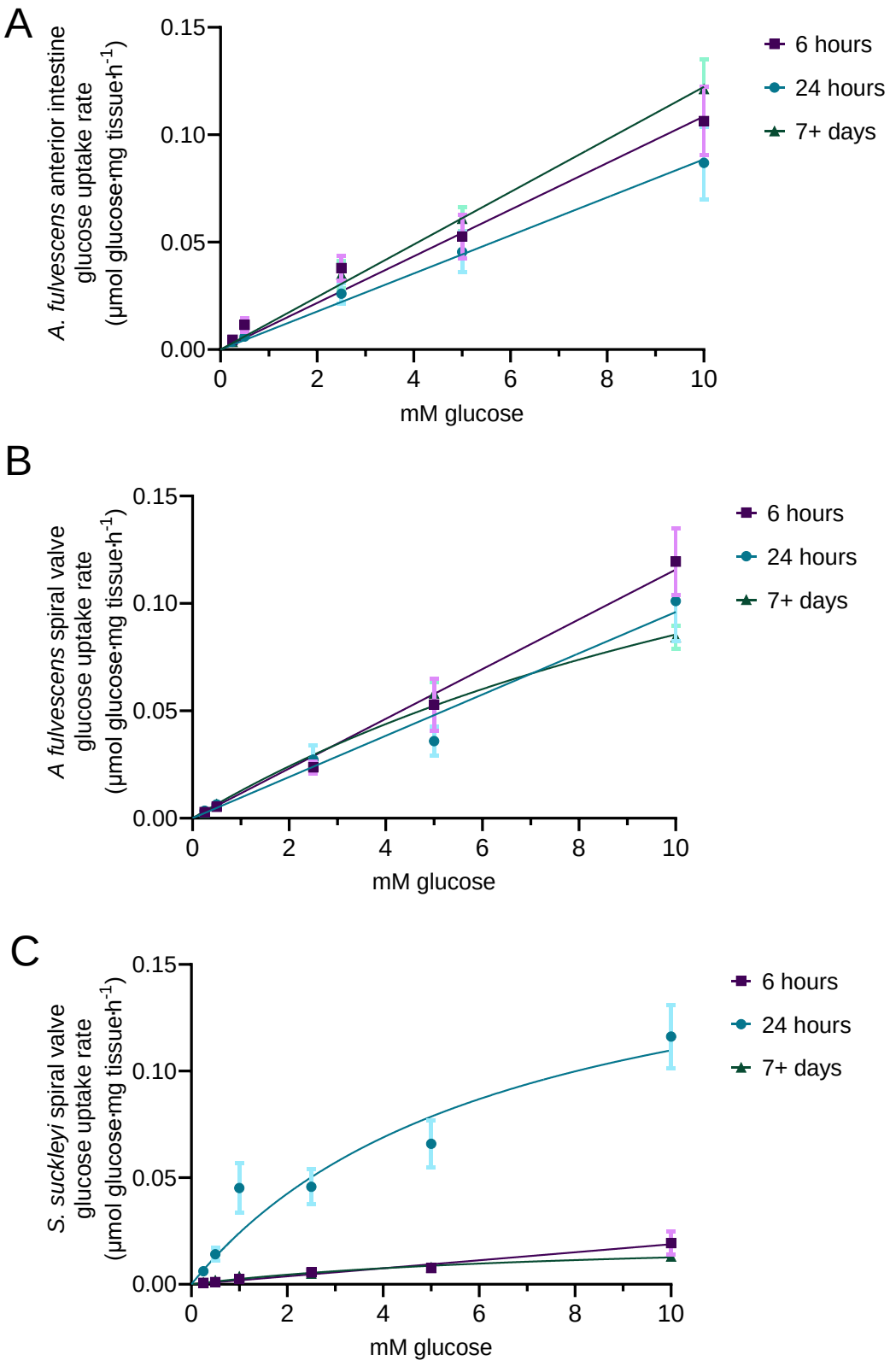
A
A. fulvescens anterior intestine
glucose uptake rate
(µmol glucose·mg tissue·h-1)
0.15
0.10
0.05
0.00
0
2
4
6
8
10
mM glucose
6 hours
24 hours
7+ days
B
A fulvescens spiral valve
glucose uptake rate
(µmol glucose·mg tissue·h-1)
0.15
0.10
0.05
0.00
0
2
4
6
8
10
mM glucose
6 hours
24 hours
7+ days
C
S. suckleyi spiral valve
glucose uptake rate
(µmol glucose·mg tissue·h-1)
0.15
0.10
0.05
0.00
0
2
4
6
8
10
mM glucose
6 hours
24 hours
7+ days

Figure 10: Glucose-dependent kinetic curves for the anterior intestine (A; n=6-7) and spiral valve (B; n=5-7) of *Acipenser fulvescens* and the spiral valve of *Squalus suckleyi* (C; n=5-7) during a postprandial time course. Tissue glucose uptake (μmol glucose·cm^{-2}·h^{-1}) data were collected using Ussing chambers for *A. fulvescens* and modified Ussing-like chambers for *S. suckleyi*. The data are represented as means ± SEM at these post-feeding time points: 6 hours (pink squares), 24 hours (blue circles), and 7+ days (green triangles). Curves were fitted to either linear or hyperbolic models (Table 5).

Table 8: Summary of linear and hyperbolic regressions of concentration dependent *in vitro* intestinal tissue uptake rate (μmol glucose·mg tissue·h^{-1}) and corresponding sum-of-squares *F* tests (null hypothesis=linear model, alternative hypothesis=hyperbolic model) during different post-feeding timepoints in *Squalus suckleyi* and *Acipenser fulvescens*.

Species	Time post-fed	GIT Region	*F*	Degrees of Freedom (Den, Ded)	*p*	Linear R^2	Hyperbolic R^2
A. fulvescens	6 hours	anterior intestine	0.7308	1, 33	0.3988	0.7172	0.7233
A. fulvescens	24 hours	anterior intestine	0.2381	1, 28	0.6294	0.6973	0.6998
A. fulvescens	7+ days	anterior intestine	0.1845	1, 28	0.6708	0.8702	0.871
A. fulvescens	6 hours	spiral valve	N/A	N/A	N/A	0.7912	ambiguous fit
A. fulvescens	24 hours	spiral valve	N/A	N/A	N/A	0.7158	ambiguous fit
A. fulvescens	7+ days	spiral valve	10.41	1, 27	0.0033	0.9092	0.9345
S. suckleyi	6 hours	spiral valve	N/A	N/A	N/A	0.6353	ambiguous fit
S. suckleyi	24 hours	spiral valve	7.574	1, 34	0.0094	0.6055	0.6774
S. suckleyi	7+ days	spiral valve	8.936	1, 40	0.0048	0.6574	0.72

Table 9: K_m (mM glucose) and V_{max} (µmol glucose·mg tissue·h^{-1}) for intestinal glucose kinetic curves during different post-feeding timepoints in *Squalus suckleyi* and *Acipenser fulvescens.*

Species	Time post-fed	GIT Region	K_m (mM glucose; glucose disappearance)	V_{max} (µmol glucose·mg tissue·h^{-1}; glucose disappearance)	K_m (mM glucose; tissue uptake)	V_{max} (µmol glucose·mg tissue·h^{-1}; tissue uptake)
A. fulvescens	6 hours	anterior intestine	N/A	N/A	N/A	N/A
A. fulvescens	24 hours	anterior intestine	N/A	N/A	N/A	N/A
A. fulvescens	7+ days	anterior intestine	N/A	N/A	N/A	N/A
A. fulvescens	6 hours	spiral valve	N/A	N/A	N/A	N/A
A. fulvescens	24 hours	spiral valve	N/A	N/A	N/A	N/A
A. fulvescens	7+ days	spiral valve	N/A	N/A	17.33	0.2337
S. suckleyi	6 hours	spiral valve	N/A	N/A	N/A	N/A
S. suckleyi	24 hours	spiral valve	N/A	N/A	6.533	0.1814
S. suckleyi	7+ days	spiral valve	17.52	1.112	8.188	0.02298

3.3.1 Sodium and SGLT1 dependent *in vitro* intestinal fluxes:

In *A. fulvescens* neither the low sodium Ringer's or phlorizin treatments impacted intestinal glucose uptake (Figure 11 and Table 10). *S. suckleyi* glucose uptake was similarly not impacted by the low sodium treatment (Figure 12 and Table 11). Phlorizin was not administered to *S. suckleyi*.

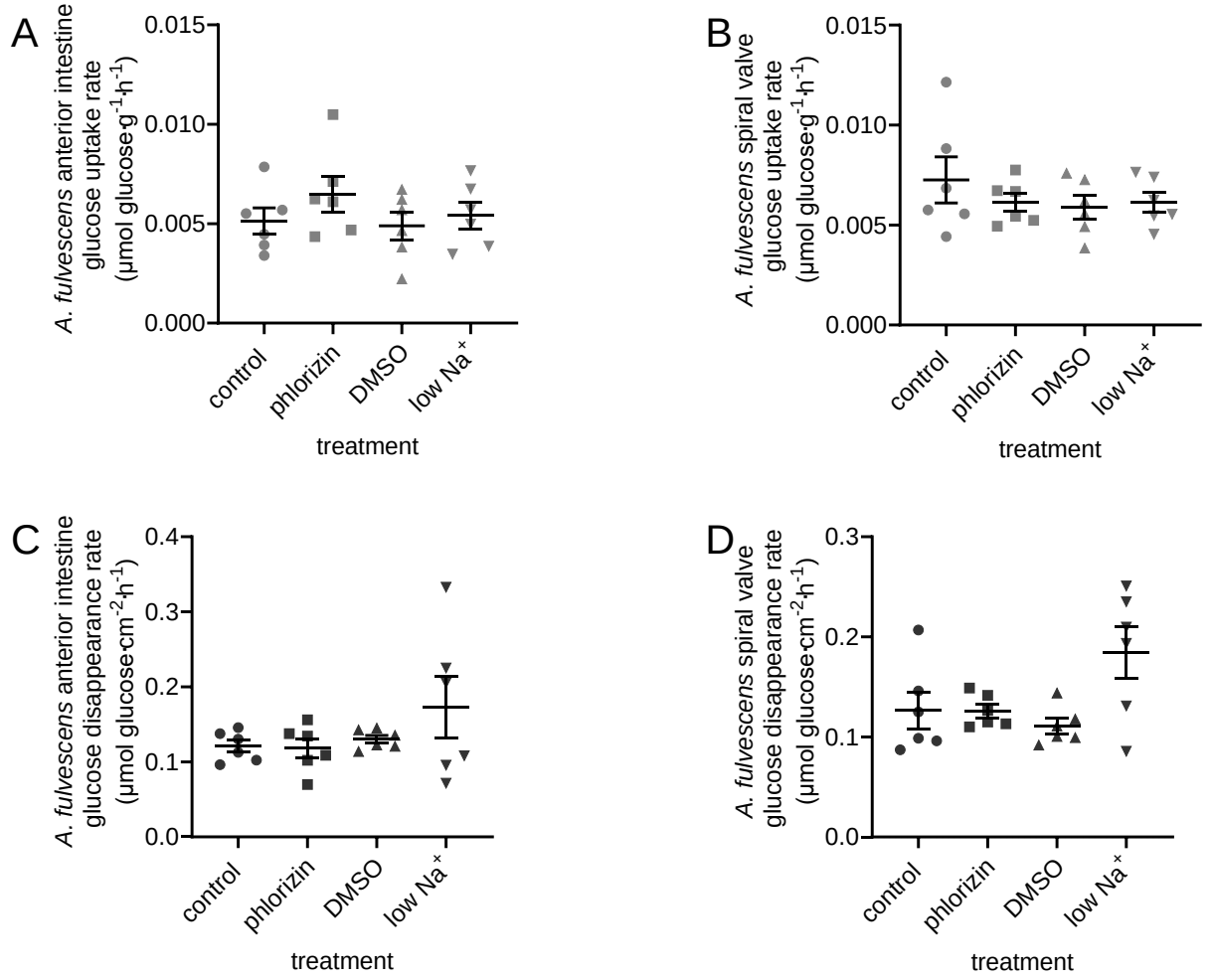

Figure 11: The impact of the SGLT1 inhibitor phlorizin and low sodium Ringer's on sodium-dependent glucose uptake in 24 hours post-fed *Acipenser fulvescens*. Tissue glucose uptake (µmol glucose $\cdot cm^{-2} \cdot h^{-1}$) in the anterior intestine (A; n=6) and spiral valve (B; n=6), and glucose disappearance rates (µmol glucose $\cdot cm^{-2} \cdot h^{-1}$) in the anterior intestine (C; n=6) and spiral valve (D; n=6) were collected with Ussing chambers; they are represented as means ± SEM. Data was analyzed using unpaired t-tests. There was no statistical significance in any treatment groups.

Table 10: Statistical summary table of the impact of the SGLT1 inhibitor phlorizin and low sodium Ringer's on sodium-dependent glucose uptake in *Acipenser fulvescens*.

Graph	GIT Region	Transformation Used	Statistical Test	*F*	Degrees of Freedom (DFn, DFd)	*p*	R^2	Kruskal-Wallis statistic (*H*)
A	anterior intestine	N/A	1-way ANOVA	0.931	3, 20	0.4439	0.1226	N/A
B	spiral valve	square root	1-way ANOVA	0.605	3, 20	0.6195	0.0832	N/A
C	anterior intestine	N/A	Kruskal-Wallis	N/A	N/A	0.8265	N/A	0.8954
D	spiral valve	inverse	1-way ANOVA	2.211	3, 20	0.1184	0.249	N/A

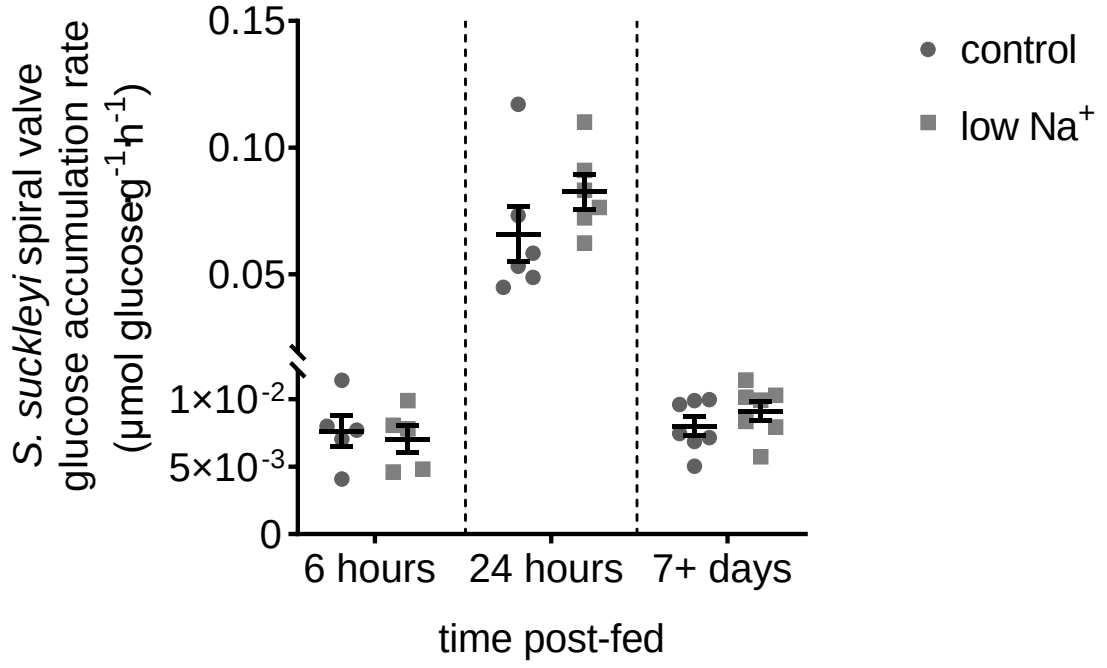

Figure 12: The impact of low sodium Ringer's on sodium-dependent glucose uptake in *Squalus suckleyi* during a postprandial timeseries. Tissue glucose uptake (µmol glucose $\cdot cm^{-2} \cdot h^{-1}$) was collected with modified Ussing-like chambers; they are represented as means ± SEM in control (circles) and low sodium (squares). Data was analyzed using unpaired t-tests. Dotted lines indicate separation in statistical tests. There was no statistical significance between any treatments.

Table 11: Statistical summary table of the impact of low sodium Ringer's on sodium-dependent glucose uptake in *Squalus suckleyi*.

Time post-fed	Transformation Used	Statistical Test	*F*	Degrees of Freedom (DFn, DFd)	*p*	R^2
6 hours	N/A	unpaired t-test	1.317	4, 4	0.7076	0.01855
24 hours	N/A	unpaired t-test	2.623	5, 5	0.2265	0.1424
7+ days	N/A	unpaired t-test	1.026	6, 6	0.289	0.09301

4.0.0 Discussion:

The intestinal spiral valve is thought to slow down the passage of chyme and increase the mucosal surface area for enhanced nutrient absorption (Bakke et al., 2010; Buddington & Christofferson, 1985) suggesting that this section of the intestine has evolved to be the primary site of nutrient uptake in fishes that possess it (Bucking, 2015; Venero et al., 2015). However, these assumptions are primarily based on morphology and there is a gap in the literature regarding its functional role. In this thesis, I examined carbohydrate digestive and transport mechanisms along the gastrointestinal tracts of *A. fulvescens* and *S. suckleyi*, two species that have a spiral valve in their GIT. Furthermore, I compared glucose uptake during a postprandial timeseries to determine if feeding induced an upregulation of transport mechanisms associated with nutrient acquisition in both species. In most gastrointestinal regions, the brush border disaccharidase, maltase, increased activity in response to feeding in both species. However, the mRNA transcript abundance of *sglt1* did not change in *A. fulvescens* in response to feeding but did in *S. suckleyi*. Finally, glucose uptake rates did not reach saturation in *A. fulvescens,* suggesting that both the anterior intestine and spiral valve play roles in glucose acquisition, rejecting the notion that the spiral valve in these fishes is the sole primary site of nutrient uptake.

4.1.0 Maltase activity

In all spiral valve regions in *A. fulvescens* and in the anterior spiral valve of *S. suckleyi*, I found higher maltase activity in the epithelial scrapings than in the underlying tissue layer. This suggests that maltase is primarily located in the intestinal brush border. Maltase is similarly considered a brush border enzyme in all other vertebrates thus far investigated (Eichholz & Crane, 1965; Miller & Crane, 1961; Sala-Rabanal et al., 2004; Sørensen et al., 1982; Tengjaroenkul et al., 2000; Ugolev, A. M. & Kuz'mina, 1994), notably including the European catshark (*Scyliorhinus canicula*; Crane et al., 1979). However, in the mid and posterior spiral valve of *S. suckleyi* there were no differences in maltase activity between the different tissue layers, suggesting significant maltase presence in the underlying tissue in addition to the brush border. This contradicts previous findings which visualized maltase in the brush border epithelium (Tengjaroenkul et al., 2000) and studies that primarily determined maltase activity in isolated brush border microvilli (Eichholz & Crane, 1965; Miller & Crane, 1961). However, the

detectable maltase activity in the underlying tissue of *S. suckleyi* could be an artifact of the tissue preparation procedure, where residual epithelial cells may have remained intact following scraping, particularly since the epithelia of *S. suckleyi* is coated with thick mucus. Remnant epithelial tissue would then contribute toward maltase activity in the underlying tissue providing, in essence, a false positive.

The highest mean intestinal maltase activity in *A. fulvescens* was approximately 3.5 fold higher than that in *S. suckleyi.* Despite both being carnivorous species, these results indicate that there is likely a higher reliance on carbohydrates in *A. fulvescens* than *S. suckleyi. A. fulvescens* are considered to have delayed sexual maturity and are typically characterized as adults when they reach a fork length over 100 cm (Bruch, 1999; Smith & Baker, 2005). The juvenile (>100 cm) fish used in this study need energy to grow and mature and therefore could benefit from an increased ability to break down and absorb dietary carbohydrates. Especially since glucose and its metabolic intermediates are required for ATP production, nucleotide (Lane & Fan, 2015), and lipid synthesis (Higgins et al., 1981). Wilson (1994) suggests that fish need appropriate amounts of dietary carbohydrates for energy and production of metabolic intermediates so that lipids and proteins don't need to be catabolized. Furthermore, carnivorous fish have shown a reliance on carbohydrates for growth. For example, the absence of dietary carbohydrates in the carnivorous rainbow trout (*Oncorhynchus mykiss*) caused muscular hypotrophy resulting in a significant depression in growth rate (Peragón et al., 1999). However, it should be noted that excess dietary carbohydrates can have negative impacts by reducing fish growth rates (Hemre et al., 2002). All considered, juvenile *A. fulvescens* may require more dietary carbohydrates than adult *S. suckleyi* to grow to maturity. Regardless, the data show regional changes in maltase activity as a function of time in both species.

When I examined the impact of feeding on gastrointestinal regional maltase activity, although relatively low compared to other gastrointestinal regions, there was a significant increase 7+ days post-feeding in the pyloric stomach of *S. suckleyi.* In the earlier timepoints it is likely that the epithelial tissues had already utilised maltase to assist in the chemical digestion of carbohydrates in the stomach. Increased activity of maltase at 7+ days post-feeding may be due to the tissues replenishing epithelial maltase stores in preparation for the next meal. While it may be unusual to record changes in carbohydrase activity in the stomach of the GIT in vertebrates, it

is important to note that many fishes have a secretory region in the stomach. The pyloric stomach acts as the secretory region, while the cardiac stomach is mostly responsible for physical digestion (Bakke et al., 2010). Thus, it is reasonable to anticipate some level of maltase activity in the pyloric stomach of *S. suckleyi*. A similar increase in maltase activity was observed in one-year-old *A. fulvescens* at the 7+ days post-feeding timepoint. However, these animals were much smaller than *S. suckleyi* and it was anatomically challenging to separate the cardiac from the pyloric stomach, so I cannot determine if the observed increase in maltase activity is localised to the pyloric stomach as observed in *S. suckleyi*.

In both species examined, I observed significantly increased maltase activity in response to feeding in the more anterior regions of the intestine: pyloric ceca and anterior intestine for *A. fulvescens* and the anterior and mid spiral valve regions for *S. suckleyi*. The observed increases in maltase activity approximately coincide with the progression of chyme along the length of the intestine. Furthermore, in both species, maltase activity in the posterior regions of the intestine was relatively low compared to the anterior regions of the intestine; a pattern that is typical in fishes previously examined (Harpaz and Uni, 1999; Krogdahl & Bakke-McKellep, 2005; Tengjaroenkul et al., 2000). Additionally, there were no postprandial changes in maltase activity in the posterior spiral valve and colon in *S. suckleyi,* nor in the anterior spiral valve of *A. fulvescens*. In contrast to *S. suckleyi,* maltase activity changed in the posterior spiral valve in *A. fulvescens* following feeding. These regional differences in maltase activity indicate heterogeneity in function along the length of the intestine which varies depending on species. The lack of significant changes in maltase activity post-feeding may suggest reduced functional relevance of carbohydrate digestion in that section. The heightened levels of maltase activity in the pyloric ceca and anterior intestine of *A. fulvescens* suggests a greater reliance on these regions for carbohydrate digestion which was also demonstrated in Atlantic salmon (*Salmo salar*; Krogdahl & Bakke-McKellep, 2005). Additionally, a previous study in the bonnethead shark (*Sphyrna tiburo*) reported high maltase activity in the anterior intestine (Jhavari et al., 2015), similar to the heightened maltase activity in the anterior spiral valve in *S. suckleyi*. Importantly, the anterior intestine in *S. suckleyi* is virtually non-existent. Therefore, the anterior spiral valve may be the primary site of glucose acquisition if there is a positive correlation between maltase activity and carbohydrate uptake in *S. suckleyi* as has been described for other

fishes (Krogdahl & Bakke-McKellep, 2005). Examination of regional abundance of key nutrient transporters would provide support for this notion.

4.2.0 *sglt1* mRNA transcript abundance:

Within the intestine, SGLT1 is a glucose transport protein present in the apical membrane of enterocytes (Suzuki et al., 2001; Yoshida et al., 1995). At 6 hours post-feeding there was a significant increase in *sglt1* mRNA transcript abundance in all spiral valve regions compared to the cardiac stomach, pyloric stomach, and colon in *S. suckleyi*. Furthermore, the abundance of *sglt1* in the spiral valve was at least 8 times greater than in the other sampled regions. This combined with the maltase activity data is indicative of the regional functional relevance of the spiral valve in carbohydrate acquisition relative to other gastrointestinal regions in *S. suckleyi*. Regional functionality was further demonstrated when comparing the changes in *sglt1* mRNA abundance post-feeding, where only the mid-spiral valve region increased 24 hours post-feeding. Intestinal regionality of *sglt1* mRNA abundance has been previously demonstrated in a variety of teleosts, with higher levels typically in the anterior regions of the intestine relative to the posterior regions (Kamalam et al., 2013; Sala-Rabanal et al., 2004; Syakuri et al., 2019).

Evidence in mammals suggests that urea uptake can be facilitated through SGLT1 (Leung et al., 2000). As elasmobranchs are nitrogen limited (Wright & Wood, 2015), the observed increase in *sglt1* abundance post-feeding may have a dual purpose of facilitating urea uptake, along with increasing glucose acquisition. Previous postprandial stable isotope analysis of *S. suckleyi* demonstrated an increase in ^{15}N labelled ammonia, urea, and glutamine in the anterior spiral valve 20 hours post-feeding (Hoogenboom & Anderson 2023). It was proposed that the increased glutamine and ammonia would be converted to urea through the ornithine urea cycle and the subsequent urea would enter the blood to support the osmoregulatory strategy of marine elasmobranchs. Urea synthesis is energetically costly (Anand & Anand, 1993), therefore accessibility to available glucose following a meal may aid urea uptake and thus nitrogen retention in these fish.

While the increase in *sglt1* mRNA transcript abundance 24 hours post-feeding may facilitate transport of other molecules, it also supports the feeding strategy of *S. suckleyi* as opportunistic predators (Jones & Geen, 1977; Compagno, 1984). Similar changes in transcript

abundance have been shown in other species that also follow an opportunistic feeding strategy and is perhaps best illustrated in the massive changes observed in the intestinal architecture of the Burmese python, *(Python bivitatus*) following a feeding event *(*Secor & Diamond, 1995; Secor & Diamond, 1998), a phenomenon that has also been demonstrated in Atlantic salmon (Krogdahl & Bakke-McKellep, 2005).

In contrast to the changes in *sglt1* mRNA abundance in *S. suckleyi*, no changes were detected in transcript abundance following feeding in *A. fulvescens*. This may be explained by the feeding ecology of this species. As benthic generalists (Chiasson et al., 1997; Nilo et al., 2006; Smith & King, 2005), *A. fulvescens* are constantly foraging on the riverbed, particularly during early life history when there is a need for rapid growth during summer months. Thus, there are likely few periods when the intestine is empty. Though not taken from the wild, the *A. fulvescens* used in the present study were hatchery reared and fed a diet of commercial trout pellets at a predictable time every day. Therefore, it would not be energetically favourable to continually up- and downregulate nutrient acquisition mechanisms.

4.3.0 *in vitro* intestinal fluxes:

In vitro experiments were conducted to determine the impact of feeding state on glucose uptake kinetics. Comparable concentration ranges were used between both species. However, this concentration range did not allow me to determine Michaelis-Menten kinetic parameters for *A. fulvescens* since the data overall fit linear over hyperbolic models. As more substrate (i.e. glucose) is added, the transport rate linearly increases with substrate concentration until the maximal rate of transport (V_{max}) is achieved. At V_{max}, the transport proteins are saturated with substrate and transport rate no longer increases with substrate concentration. Therefore, in order to calculate K_m (substrate concentration at which the transport rate is half of V_{max}) and V_{max}, a hyperbolic curve is necessary. Therefore, I was unable to determine the impact of feeding on glucose acquisition in *A. fulvescens*. Since transport saturation wasn't reached in the anterior intestine and spiral valve of *A. fulvescens,* it suggests that both tissues are capable of absorbing large quantities of glucose. It additionally suggests that the anterior intestine plays a large role in glucose uptake alongside the spiral valve. The significant role of the anterior intestine in carbohydrate acquisition is also corroborated by the maltase and *sglt1* data. To achieve transport

saturation, I likely needed higher glucose concentrations as reported in white sturgeon (*Acipenser transmontanus*; Buddington et al., 1987). Regardless, the ability of these carnivorous fish to absorb much larger glucose quantities than they would encounter in their diets is intriguing since, in comparison, carnivorous teleosts are often termed as being glucose intolerant (Moon, 2001). Alternatively, Michaelis-Menten kinetics for glucose uptake were determined in *S. suckleyi* at 24 hours and 7+ days post-feeding. There was a significant decrease in V_{max} 7+ days post-feeding, indicative of a reduction in glucose acquisition mechanisms once food had cleared the GIT. Previous studies indicate that *S. suckleyi* clear the majority of food from their GIT approximately five days post-feeding (Jones & Geen, 1977; Wood et al., 2007). Thus, *S. suckleyi* downregulating intestinal glucose transport mechanisms in a fasted state (7+ days post-feeding) provides a physiological connection to the observed opportunistic feeding strategy of these fish (Compagno, 1984; Jones & Geen, 1977), again indicating variable regulation of transport mechanisms in response to satiated state as described in other vertebrates (Papastamatiou & Lowe, 2005; Secor & Diamond, 1995; Secor & Diamond, 1998). On the other hand, a recent study examining pancreas function in *S. suckleyi* in response to feeding demonstrated no change in pancreatic lipase, trypsin, and carbohydrase activities between fed and fasted fish, suggesting the pancreas is constantly prepared for food intake (Weinrauch et al., 2022b). The observed differences in preparedness for digestion of a meal between the pancreas and intestine may be due to the exocrine pancreas storing enzymes in intracellular zymogen granules in acinar cells (Gage, 1943; Logsdon, 2004). Depleted zymogen stores would not be ideal during a feeding event.

4.3.1 Sodium and SGLT1 dependent *in vitro* intestinal fluxes:

In both species, a significant reduction of sodium from Ringer's solutions did not inhibit intestinal radiolabelled glucose uptake. This does not align with the literature which supports sodium-dependent glucose uptake in fishes and other vertebrates (Ahearn et al., 1992; Kunio et al., 1983; Subramaniam et al., 2019). SGLT1 was initially identified as a sodium-dependent glucose transport protein but has since demonstrated the ability to utilize other cations to facilitate glucose transport in mammals (Wright et al., 2003). The promiscuity of SGLT1 may have enabled similar levels of glucose transport to occur between the reduced sodium and control treatment groups. Alternatively, remaining intestinal mucus in the tissue preparations of both

species may have provided sufficient sodium to facilitate glucose uptake. Other previous studies have used isolated brush border membrane vesicles to demonstrate sodium dependence on glucose uptake (Ahearn et al., 1992; Kunio et al., 1983), which would eliminate problems relating to mucus.

In *A. fulvescens,* phlorizin was also administered to inhibit glucose uptake. Phlorizin is a classical competitive inhibitor that, in mammals, binds to the phlorizin binding pocket in C-terminal loop 13 to induce a confirmational change in SGLT1 (Raja & Kinne, 2015). Binding of phlorizin has been used to successfully infer abundance of active SGLT1 transport proteins (Ferraris & Diamond, 1986; Herrmann et al., 2016) due to its role as an effective competitive inhibitor. Phlorizin has also previously shown evidence of significantly reducing glucose transport in fish (Ahearn et al., 1992; Maffia et al., 1996; Subramaniam et al., 2019), though the biochemical properties of this interaction are less studied in fish than in mammals. The findings in this study do not match the literature since phlorizin did not inhibit glucose uptake in *A. fulvescens.* Wimmer et al. (2008) demonstrated that D-glucose and L-glucose reduced phlorizin binding in the C-terminal loop 13 in a nonspecific competitive manner in mammals. The relatively high concentration (5 mM) of glucose in the mucosal Ringer's solution used in this study may have resulted in glucose outcompeting phlorizin to bind to the binding pocket in *A. fulvescens*. Transport of a radiolabelled non-metabolizable glucose analog methylglucose (3-OMG) in the common carp (*Cyprinus carpio*) epithelioma papulosum cyprinid cell line was only inhibited by very high phlorizin concentrations (1 mM; Teerijoki et al., 2001). A higher phlorizin concentration might have led to glucose transport inhibition in this study. Kellett (2001) suggests that increasing glucose concentrations induce SGLT1 to activate intracellular protein kinase C and MAPK signalling pathways, resulting in the rapid trafficking GLUT2 transport proteins to the apical brush border membrane. Since GLUT2 is not inhibited by phlorizin, the lack of phlorizin inhibition on glucose transport in *A. fulvescens* could be attributed to the potential trafficking of GLUT2 to the apical membrane.

4.5.0 Conclusions:

By comparing mechanisms associated with glucose acquisition in two phylogenetically distant organisms with different feeding strategies (*A. fulvescens* and *S. suckleyi*), I provided

insight into the relative role of the spiral valve. Evidence of changes in the regulation of glucose transport mechanisms was found in the more opportunistically feeding *S. suckleyi* compared to the continuously feeding *A. fulvescens.* This indicates that feeding strategies may influence the intestinal responses of organisms with a spiral valve. Additionally, *A. fulvescens* does not primarily rely on the spiral valve for the digestion of carbohydrates and uptake of glucose, it also utilizes the anterior intestine for these processes. In contrast, S. suckleyi predominantly carries out these activities in the spiral valve, indicating a distinct variation in the relative role of the spiral valve between the two species. Furthermore, this study provided evidence of functional specialization within the spiral valve of some species, as seen by regional changes in *sglt1* mRNA abundance in *S. suckleyi*. This study also underscores the importance of comparing morphology to physiology in order to fully understand the functional role of an organ.

4.6.0 Future directions:

Issues were encountered scraping tissues to determine localization of enzyme activity in *S. suckleyi.* If I was able to determine maltase intratissue localization in the future, a better methodology would be to use enzyme histochemistry as seen in Tengjaroenkul et al. (2000). This would allow for a visual determination of maltase localization that would not be impeded by the drawbacks of scraping tissues. For the *sglt1* mRNA abundance, I am unable to directly correlate increases in mRNA transcript abundance with the translation of transport proteins. Thus, while increased transcript abundance may be indicative of increased protein expression without the measurement of the protein, I cannot definitively say there is a change in function of the tissue. In the future it would be interesting to utilize immunohistochemistry to visualize changes in SGLT1 protein abundance based on location and/or timing post-feeding in both species.

Mucus likely had an impact on the results throughout this study. Gastrointestinal mucus in mammals is composed of an easily removable outer layer and a more firmly adherent underlying layer, with the thickness of each layer varying along the tract (Atuma et al., 2001). If this mucus structure is similar in fish with a firmly adherent underlying layer along the GIT, it would explain the difficulty in fully removing gastrointestinal mucus from the samples in this study. Loosely adherent mucus is quickly regenerated by goblet cells after removal (Atuma et al., 2001). The presence of goblet cells makes the task of completely separating out mucus near

futile. It should be noted that mammalian mucus composition (Johansson et al., 2011; Rodríguez-Piñeiro et al., 2013) and thickness (Atuma et al., 2001) is not homogenous along the gastrointestinal tract. If this holds true in fish, it could play a role in gastrointestinal functional regionality. Additionally, research has demonstrated increasing complexity in form and structure of gastrointestinal mucins along the GIT in vertebrates (Lang et al., 2004) and these differences will impact nutrient uptake. The role of mucins and the mucosal layer(s) in nutrient acquisition in the GIT of fishes is largely unexplored and should be investigated in the future to provide a more comprehensive understanding of nutrient acquisition.

This study examined gastrointestinal carbohydrate acquisition. Future studies could similarly examine lipid and protein acquisition to provide a more comprehensive understanding of nutrient acquisition in these organisms. There currently is not a lot known about the spiral valve and nutrient acquisition and its emergence in evolutionary history. Though a two-species comparison can be useful to begin to understand a phenomenon, this study does not capture the full scope of even organisms within the taxa which they are designated. To understand the emergence and subsequent loss of the spiral valve, more species with spiral valves need to be examined.

6.0.0 Literature Cited:

Ahearn, G. A., Behnke, R. D., Zonno, V. and Storelli, C. (1992). Kinetic heterogeneity of Na-D-glucose cotransport in teleost gastrointestinal tract. *American Journal of Physiology-Regulatory, Integrative and Comparative Physiology* **263**, R1018–R1023.

Allen, P. J., Barth, C. C., Peake, S. J., Abrahams, M. V. and Anderson, W. G. (2009). Cohesive social behaviour shortens the stress response: the effects of conspecifics on the stress response in lake sturgeon *Acipenser fulvescens*. *Journal of Fish Biology* **74**, 90–104.

Anand, U. and Anand, C. (1993). The energy cost of urea synthesis. *Biochemical Education* **21**, 198–199.

Anderson, W.G., McCabe, C., Brandt, C. and Wood, C. M. (2015). Examining urea flux across the intestine of the spiny dogfish, *Squalus acanthias*. *Comparative Biochemistry and Physiology Part A: Molecular & Integrative Physiology* **181**, 71–78.

Argyriou, T., Clauss, M., Maxwell, E. E., Furrer, H. and Sánchez-Villagra, M. R. (2016). Exceptional preservation reveals gastrointestinal anatomy and evolution in early actinopterygian fishes. *Scientific Reports* **6**, 1–10.

Atuma, C., Strugala, V., Allen, A. and Holm, L. (2001). The adherent gastrointestinal mucus gel layer: thickness and physical state in vivo. *American Journal of Physiology-Gastrointestinal and Liver Physiology* **280**, G922–G929.

Bakke, A. M., Glover, C. and Krogdahl, Å. (2010). 2 - Feeding, digestion and absorption of nutrients. In *Fish Physiology* (ed. Grosell, M., Farrell, A. P., and Brauner, C. J.), pp. 57–110. Academic Press.

Bakke-McKellep, A. M., Nordrum, S., Krogdahl, Å. and Buddington, R. K. (2000). Absorption of glucose, amino acids, and dipeptides by the intestines of Atlantic salmon (*Salmo salar L.*). *Fish Physiology and Biochemistry* **22**, 33–44.

Ballantyne, J. S. (1997). Jaws: The Inside Story. The Metabolism of Elasmobranch Fishes. *Comparative Biochemistry and Physiology Part B: Biochemistry and Molecular Biology* **118**, 703–742.

Blasco, J., Fernàndez-Borràs, J., Marimon, I. and Requena, A. (1996). Plasma glucose kinetics and tissue uptake in brown trout in vivo: effect of an intravascular glucose load. *The Journal of Comparative Physiology B: Biochemical, Systemic, and Environmental Physiology* **165**, 534–541.

Bruch, R. M. (1999). Management of lake sturgeon on the Winnebago System - long term impacts of harvest and regulations on population structure. *Journal of Applied Ichthyology* **15**, 142–152.

Bucking, C. (2015). 6 - Feeding and Digestion in Elasmobranchs: Tying Diet and Physiology Together. In *Fish Physiology* (ed. Shadwick, R. E., Farrell, A. P., and Brauner, C. J.), pp. 347–394. Academic Press.

Buddington, R. K. (1985). Digestive secretions of lake sturgeon, *Acipenser fulvescens*, during early development. *Journal of Fish Biology* **26**, 715–723.

Buddington, R. K., Chen, J. W. and Diamond, J. (1987). Genetic and phenotypic adaptation of intestinal nutrient transport to diet in fish. *The Journal of Physiology* **393**, 261–281.

Buddington, R. K. and Christofferson, J. P. (1985). Digestive and feeding characteristics of the chondrosteans. *Environmental Biology of Fishes* **14**, 31–41.

Buddington, R. K. and Diamond, J. M. (1987). Pyloric ceca of fish: a "new" absorptive organ. *American Journal of Physiology-Gastrointestinal and Liver Physiology* **252**, G65–G76.

Buddington, R. K. and Doroshov, S. I. (1986). Digestive enzyme complement of white sturgeon (*Acipenser transmontanus*). *Comparative Biochemistry and Physiology Part A: Physiology* **83**, 561–567.

Caccia, S., Casartelli, M., Grimaldi, A., Losa, E., de Eguileor, M., Pennacchio, F. and Giordana, B. (2007). Unexpected similarity of intestinal sugar absorption by SGLT1 and apical GLUT2 in

an insect (*Aphidius ervi*, Hymenoptera) and mammals. *American Journal of Physiology-Regulatory, Integrative and Comparative Physiology* **292**, R2284–R2291.

Canback, B., Andersson, S. G. E. and Kurland, C. G. (2002). The global phylogeny of glycolytic enzymes. *Proceedings of the National Academy of Sciences of the United States of America* **99**, 6097–6102.

Cant, J. P., McBride, B. W. and Croom, W. J. (1996). The regulation of intestinal metabolism and its impact on whole animal energetics. *Journal of Animal Science* **74**, 2541.

Carrier, J. C., Musick, J. A. and Heithaus, M. R. (2012). *Biology of Sharks and Their Relatives*. Baton Rouge, United States: Taylor & Francis Group.

Castillo, J., Crespo, D., Capilla, E., Díaz, M., Chauvigné, F., Cerdà, J. and Planas, J. V. (2009). Evolutionary structural and functional conservation of an ortholog of the GLUT2 glucose transporter gene (SLC2A2) in zebrafish. *American Journal of Physiology-Regulatory, Integrative and Comparative Physiology* **297**, R1570–R1581.

Chan, A. S., Horn, M. H., Dickson, K. A. and Gawlicka, A. (2004). Digestive enzyme activities in carnivores and herbivores: comparisons among four closely related prickleback fishes (Teleostei: Stichaeidae) from a California rocky intertidal habitat. *Journal of Fish Biology* **65**, 848–858.

Chatchavalvanich, K., Marcos, R., Poonpirom, J., Thongpan, A. and Rocha, E. (2006). Histology of the digestive tract of the freshwater stingray *Himantura signifer* Compagno and Roberts, 1982 (Elasmobranchii, Dasyatidae). *Anatomy and Embryology* **211**, 507–518.

Cheeseman, C. I. (1993). GLUT2 is the transporter for fructose across the rat intestinal basolateral membrane. *Gastroenterology* **105**, 1050–1056.

Chen, Y.-J., Zhang, T.-Y., Chen, H.-Y., Lin, S.-M., Luo, L. and Wang, D.-S. (2017). Simultaneous stimulation of glycolysis and gluconeogenesis by feeding in the anterior intestine of the omnivorous GIFT tilapia, *Oreochromis niloticus*. *Biology Open* **6**, 818–824.

Chiasson, W. B., Noakes, D. L. and Beamish, F. W. H. (1997). Habitat, benthic prey, and distribution of juvenile lake sturgeon (*Acipenser fulvescens*) in northern Ontario rivers. *Canadian Journal of Fisheries and Aquatic Sciences* **54**, 2866–2871.

Cohen, M., Kitsberg, D., Tsytkin, S., Shulman, M., Aroeti, B. and Nahmias, Y. (2014). Live imaging of GLUT2 glucose-dependent trafficking and its inhibition in polarized epithelial cysts. *Open Biology* **4**, 140091.

Compagno, L.J.V. (1984). Sharks of the world. An annotated and illustrated catalogue of shark species known to date. Part 1. Hexanchiformes to Lamniformes. FAO Fish Synop. 125:1-249.

Cox, S. E. (2013). Energy Metabolism. In *Encyclopedia of Human Nutrition (Third Edition)* (ed. Caballero, B.), pp. 177–185. Waltham: Academic Press.

Crane, R. K., Boge, G. and Rigal, A. (1979). Isolation of brush border membranes in vesicular form from the intestinal spiral valve of the small dogfish (*Scyliorhinus canicula*). *Biochimica et Biophysica Acta (BBA) - Biomembranes* **554**, 264–267.

Daprà, F., Gai, F., Palmegiano, G. B., Sicuro, B., Falzone, M., Cabiale, K. and Galloni, M. (2009). Siberian sturgeon (*Acipenser baeri*, Brandt JF 1869) gut: anatomic description *International Aquatic Research* **16**.

Darriba, S., San Juan, F. and Guerra, A. (2005). Energy storage and utilization in relation to the reproductive cycle in the razor clam *Ensis arcuatus* (Jeffreys, 1865). *ICES Journal of Marine Science* **62**, 886–896.

Deck, C. A., Anderson, W. G., Conlon, J. M. and Walsh, P. J. (2017). The activity of the rectal gland of the North Pacific spiny dogfish *Squalus suckleyi* is glucose dependent and stimulated by glucagon-like peptide-1. *The Journal of Comparative Physiology B: Biochemical, Systemic, and Environmental Physiology* **187**, 1155–1161.

Deck, C. A., LeMoine, C. M. R. and Walsh, P. J. (2016). Phylogenetic analysis and tissue distribution of elasmobranch glucose transporters and their response to feeding. *Biology Open* **5**, 256–261.

Eichholz, A. and Crane, R. K. (1965). Studies on the organization of the brush border in intestinal epithelial cells. *Journal of Cell Biology* **26**, 687–691.

Elliott, J. P. and Bellwood, D. R. (2003). Alimentary tract morphology and diet in three coral reef fish families. *Journal of Fish Biology* **63**, 1598–1609.

Fänge, R., Lundblad, G., Lind, J. and Slettengren, K. (1979). Chitinolytic enzymes in the digestive system of marine fishes. *Marine Biology* **53**, 317–321.

Ferraris, R. P. and Diamond, J. M. (1986). A method for measuring apical glucose transporter site density in intact intestinal mucosa by means of phlorizin binding. *The Journal of Membrane Biology* **94**, 65–75.

Ferraris, R. P., Lee, P. P. and Diamond, J. M. (1989). Origin of regional and species differences in intestinal glucose uptake. *American Journal of Physiology-Gastrointestinal and Liver Physiology* **257**, G689–G697.

Furné, M., García-Gallego, M., Hidalgo, M. C., Morales, A. E., Domezain, A., Domezain, J. and Sanz, A. (2008). Effect of starvation and refeeding on digestive enzyme activities in sturgeon (*Acipenser naccarii*) and trout (*Oncorhynchus mykiss*). *Comparative Biochemistry and Physiology Part A: Molecular & Integrative Physiology* **149**, 420–425.

Furné, M., Morales, A. E., Trenzado, C. E., García-Gallego, M., Carmen Hidalgo, M., Domezain, A. and Sanz Rus, A. (2012). The metabolic effects of prolonged starvation and refeeding in sturgeon and rainbow trout. *The Journal of Comparative Physiology B: Biochemical, Systemic, and Environmental Physiology* **182**, 63–76.

Furné, M. and Sanz, A. (2018). Starvation in Fish – Sturgeon and Rainbow Trout as Examples. In *Handbook of Famine, Starvation, and Nutrient Deprivation: From Biology to Policy* (ed. Preedy, V. and Patel, V. B.), pp. 1–16. Cham: Springer International Publishing.

Gage, S. H. (1943). Zymogen Granules in the Fishes. *Transactions of the American Fisheries Society* **72**, 263–266.

Gamperl, A. K. and Driedzic, W. R. (2009). Chapter 7 Cardiovascular Function and Cardiac Metabolism. In *Fish Physiology* (ed. Richards, J. G., Farrell, A. P., and Brauner, C. J.), pp. 301–360. Academic Press.

Gardiner, B. G. (1984). Sturgeons as Living Fossils. In *Living Fossils* (ed. Eldredge, N. and Stanley, S. M.), pp. 148–152. New York, NY: Springer.

German, D. P., Horn, M. H. and Gawlicka, A. (2004). Digestive enzyme activities in herbivorous and carnivorous prickleback fishes (Teleostei: Stichaeidae): ontogenetic, dietary, and phylogenetic effects. *Physiological and Biochemical Zoology* **77**, 789–804.

German, D. P., Neuberger, D. T., Callahan, M. N., Lizardo, N. R. and Evans, D. H. (2010). Feast to famine: The effects of food quality and quantity on the gut structure and function of a detritivorous catfish (Teleostei: Loricariidae). *Comparative Biochemistry and Physiology Part A: Molecular & Integrative Physiology* **155**, 281–293.

Ghezzi, C., Loo, D. D. F. and Wright, E. M. (2018). Physiology of renal glucose handling via SGLT1, SGLT2 and GLUT2. *Diabetologia* **61**, 2087–2097.

Hassanpour, M. and Joss, J. (2009). Anatomy and Histology of the Spiral Valve Intestine in Juvenile Australian Lungfish, *Neoceratodus forsteri*. *The Open Zoology Journal* **2**, 62–85.

Hediger, M. A. and Rhoads, D. B. (1994). Molecular physiology of sodium-glucose cotransporters. *Physiological Reviews* **74**, 993–1027.

Hediger, M. A., Turk, E., Pajor, A. M. and Wright, E. M. (1989). Molecular genetics of the human Na^+/glucose cotransporter. *Wiener klinische Wochenschrift* **67**, 843–846.

Hemre, G.-I., Mommsen, T. p. and Krogdahl, Å. (2002). Carbohydrates in fish nutrition: effects on growth, glucose metabolism and hepatic enzymes. *Aquaculture Nutrition* **8**, 175–194.

Hernandez-Blazquez, F. J., Guerra, R. R., Kfoury, J. R., Bombonato, P. P., Cogliati, B. and Silva, J. R. M. C. da (2006). Fat absorptive processes in the intestine of the Antarctic fish *Notothenia coriiceps* (Richardson, 1844). *Polar Biology* **29**, 831–836.

Herrmann, J., Möller, N., Lange, P. and Breves, G. (2016). Different phlorizin binding properties to porcine mucosa of the jejunum and ileum in relation to SGLT1 activity. *Journal of Animal Science* **94**, 238–242.

Higgins, T. J. C., Allsopp, D., Bailey, P. J. and D'Souza, E. D. A. (1981). The relationship between glycolysis, fatty acid metabolism and membrane integrity in neonatal myocytes. *Journal of Molecular and Cellular Cardiology* **13**, 599–615.

Höfer, D., Asan, E. and Drenckhahn, D. (1999). Chemosensory Perception in the Gut. *Physiology* **14**, 18–23.

Hoogenboom, J. L. and Anderson, W. G. (2023). Using 15N to determine the metabolic fate of dietary nitrogen in North Pacific spiny dogfish (*Squalus acanthias suckleyi*). *Journal of Experimental Biology* **226**, jeb244921.

Hossain, A.M., Dutta, H.M. (1996). Phylogeny, Ontogeny, Structure and Function of Digestive Tract Appendages (Caeca) in Teleost Fish. In *Fish Morphology*, pp. 59-76.

Hung, S. S. O. (1991). Carbohydrate utilization by white sturgeon as assessed by oral administration tests. *The Journal of Nutrition* **121**, 1600–1605.

Hung, S. S. O., Fynn-Aikins, F. K., Lutes, P. B. and Xu, R. (1989). Ability of juvenile white sturgeon (*Acipenser transmontanus*) to utilize different carbohydrate sources. *The Journal of Nutrition* **119**, 727–733.

Jhaveri, P., Papastamatiou, Y. P. and German, D. P. (2015). Digestive enzyme activities in the guts of bonnethead sharks (*Sphyrna tiburo*) provide insight into their digestive strategy and evidence for microbial digestion in their hindguts. *Comparative Biochemistry and Physiology Part A: Molecular & Integrative Physiology* **189**, 76–83.

Johansson, M. E. V., Ambort, D., Pelaseyed, T., Schütte, A., Gustafsson, J. K., Ermund, A., Subramani, D. B., Holmén-Larsson, J. M., Thomsson, K. A., Bergström, J. H., et al. (2011). Composition and functional role of the mucus layers in the intestine. *Cellular and Molecular Life Sciences* **68**, 3635–3641.

Jones, B. C. and Geen, G. H. (1977). Food and Feeding of Spiny Dogfish (*Squalus acanthias*) in British Columbia Waters. *Journal of the Fisheries Research Board of Canada* **34**, 2056–2066.

Jönsson, A.-C. (1991). Regulatory peptides in the pancreas of two species of elasmobranchs and in the Brockmann bodies of four teleost species. *Cell and Tissue Research* **266**, 163–172.

Kaitetzidou, E., Ludwig, A., Gessner, J. and Sarropoulou, E. (2017). Expression Patterns of Atlantic Sturgeon (*Acipenser oxyrinchus*) During Embryonic Development. *G3: Genes, Genomes, Genetics* **7**, 533–542.

Kamalam, B. S., Panserat, S., Aguirre, P., Geurden, I., Fontagné-Dicharry, S. and Médale, F. (2013). Selection for high muscle fat in rainbow trout induces potentially higher chylomicron synthesis and PUFA biosynthesis in the intestine. *Comparative Biochemistry and Physiology Part A: Molecular & Integrative Physiology* **164**, 417–427.

Karasov, W. H. and Douglas, A. E. (2013). Comparative Digestive Physiology. *Comprehensive Physiology* **3**, 741–783.

Kellett, G. L. (2001). The facilitated component of intestinal glucose absorption. *The Journal of Physiology* **531**, 585–595.

Krieger, J. and Fuerst, P. A. (2002). Evidence for a Slowed Rate of Molecular Evolution in the Order Acipenseriformes. *Molecular Biology and Evolution* **19**, 891–897.

Krogdahl, Å. and Bakke-McKellep, A. M. (2005). Fasting and refeeding cause rapid changes in intestinal tissue mass and digestive enzyme capacities of Atlantic salmon (*Salmo salar L.*). *Comparative Biochemistry and Physiology Part A: Molecular & Integrative Physiology* **141**, 450–460.

Krogdahl, Å., Hemre, G.-I. and Mommsen, T. P. (2005). Carbohydrates in fish nutrition: digestion and absorption in postlarval stages. *Aquaculture Nutrition* **11**, 103–122.

Krogdahl, Nordrum, Sørensen, Brudeseth, and Røsjø (1999). Effects of diet composition on apparent nutrient absorption along the intestinal tract and of subsequent fasting on mucosal

disaccharidase activities and plasma nutrient concentration in Atlantic salmon *Salmo salar L.* *Aquaculture Nutrition* **5**, 121–133.

Kumari, A. (2018). Chapter 1 - Glycolysis. In *Sweet Biochemistry* (ed. Kumari, A.), pp. 1–5. Academic Press.

Kunio, Y., Yoshimi, N. and Yoshiki, T. (1983). Effect of phloretin on Na^+-dependent D-glucose uptake by intestinal brush border membrane vesicles. *Biochemical Pharmacology* **32**, 3453–3457.

Laffel, L. (1999). Ketone bodies: a review of physiology, pathophysiology and application of monitoring to diabetes. *Diabetes/Metabolism Research and Reviews* **15**, 412–426.

Lane, A. N. and Fan, T. W.-M. (2015). Regulation of mammalian nucleotide metabolism and biosynthesis. *Nucleic Acids Research* **43**, 2466–2485.

Lang, T., Alexandersson, M., Hansson, G. C. and Samuelsson, T. (2004). Bioinformatic identification of polymerizing and transmembrane mucins in the puffer fish *Fugu rubripes*. *Glycobiology* **14**, 521–527.

Lang, T., Hansson, G. C. and Samuelsson, T. (2007). Gel-forming mucins appeared early in metazoan evolution. *Proceedings of the National Academy of Sciences* **104**, 16209–16214.

Leigh, S. C., Papastamatiou, Y. and German, D. P. (2017). The nutritional physiology of sharks. *Reviews in Fish Biology and Fisheries* **27**, 561–585.

Leung, D. W., Loo, D. D. F., Hirayama, B. A., Zeuthen, T. and Wright, E. M. (2000). Urea transport by cotransporters. *The Journal of Physiology* **528**, 251–257.

Liang, H., Ge, X., Ren, M., Zhang, L., Xia, D., Ke, J. and Pan, L. (2021). Molecular characterization and nutritional regulation of sodium-dependent glucose cotransporter 1 (Sglt1) in blunt snout bream (*Megalobrama amblycephala*). *Scientific Reports* **11**, 13962.

Logsdon, C. D. (2004). Pancreatic Enzyme Secretion (Physiology). In Encyclopedia of Gastroenterology (ed. Johnson, L. R.), pp. 68–75. New York: Elsevier.

Loo, D. D. F., Wright, E. M. and Zeuthen, T. (2002). Water pumps. *The Journal of Physiology* **542**, 53–60.

Maffia, M., Acierno, R., Cillo, E. and Storelli, C. (1996). Na(+)-D-glucose cotransport by intestinal BBMVs of the Antarctic fish *Trematomus bernacchii*. *American Journal of Physiology-Regulatory, Integrative and Comparative Physiology* **271**, R1576–R1583.

Martin, A. P., Naylor, G. J. P. and Palumbi, S. R. (1992). Rates of mitochondrial DNA evolution in sharks are slow compared with mammals. *Nature* **357**, 153–155.

Miller, D. and Crane, R. K. (1961). The digestive function of the epithelium of the small intestine: II. Localization of disaccharide hydrolysis in the isolated brush border portion of intestinal epithelial cells. *Biochimica et Biophysica Acta* **52**, 293–298.

Millikin, M. R. (1982). Qualitative and quantitative nutrient requirements of fishes: a review [Protein, amino acid, lipid, fatty acid, vitamin, mineral requirements]. *Fishery bulletin United States, National Marine Fisheries Service*.

Mommsen, T. P., Osachoff, H. L. and Elliott, M. E. (2003). Metabolic zonation in teleost gastrointestinal tract. *The Journal of Comparative Physiology B: Biochemical, Systemic, and Environmental Physiology* **173**, 409–418.

Moon, T. W. (2001). Glucose intolerance in teleost fish: fact or fiction? *Comparative Biochemistry and Physiology Part B: Biochemistry and Molecular Biology* **129**, 243–249.

Naftalin, R. J. (2014). Does apical membrane GLUT2 have a role in intestinal glucose uptake? *F1000Research* **3**, 304.

Navarro, I. and Gutiérrez, J. (1995). Chapter 17 Fasting and starvation. In *Biochemistry and Molecular Biology of Fishes*, pp. 393–434. Elsevier

Nevalenny, A. N. and Bednyakov, D. A. (2017). Distribution of the enzyme activity in the intestine of beluga *Huso huso* and Russian sturgeon *Acipenser gueldenstaedtii* (Acipenseridae). *Journal of Ichthyology* **57**, 164–169.

Nilo, P., Tremblay, S., Bolon, A., Dodson, J., Dumont, P. and Fortin, R. (2006). Feeding Ecology of Juvenile Lake Sturgeon in the St. Lawrence River System. *Transactions of the American Fisheries Society* **135**, 1044–1055.

Olsson, J., Quevedo, M., Colson, C. and Svanback, R. (2007). Gut length plasticity in perch: into the bowels of resource polymorphisms. *Biological Journal of the Linnean Society* **90**, 517–523.

Papastamatiou, Y. P. and Lowe, C. G. (2005). Variations in gastric acid secretion during periods of fasting between two species of shark. *Comparative Biochemistry and Physiology Part A: Molecular & Integrative Physiology* **141**, 210–214.

Patterson, C. (1982). Morphology and Interrelationships of Primitive Actinopterygian Fishes. *American Zoologist* **22**, 241–259.

Peragón, J., Barroso, J. B., García-Salguero, L., de la Higuera, M. and Lupiáñez, J. A. (1999). Carbohydrates affect protein-turnover rates, growth, and nucleic acid content in the white muscle of rainbow trout (*Oncorhynchus mykiss*). *Aquaculture* **179**, 425–437.

Pessin, J. E. and Bell, G. I. (1992). Mammalian facilitative glucose transporter family: structure and molecular regulation. *Annual Review of Physiology* **54**, 911–930.

Polakof, S., Mommsen, T. P. and Soengas, J. L. (2011). Glucosensing and glucose homeostasis: From fish to mammals. *Comparative Biochemistry and Physiology Part B: Biochemistry and Molecular Biology* **160**, 123–149.

Polakof, S., Panserat, S., Soengas, J. L. and Moon, T. W. (2012). Glucose metabolism in fish: a review. *The Journal of Comparative Physiology B: Biochemical, Systemic, and Environmental Physiology* **182**, 1015–1045.

Raja, M. and Kinne, R. K. H. (2015). Identification of phlorizin binding domains in sodium-glucose cotransporter family: SGLT1 as a unique model system. *Biochimie* **115**, 187–193.

Raybould, H. E. and Zittel, T. T. (1995). Inhibition of gastric motility induced by intestinal glucose in awake rats: role of Na^+-glucose co-transporter. *Neurogastroenterology & Motility* **7**, 9–14.

Redjadj, C., Darmon, G., Maillard, D., Chevrier, T., Bastianelli, D., Verheyden, H., Loison, A. and Saïd, S. (2014). Intra- and Interspecific Differences in Diet Quality and Composition in a Large Herbivore Community. *PLOS One* **9**, e84756.

Röder, P. V., Geillinger, K. E., Zietek, T. S., Thorens, B., Koepsell, H. and Daniel, H. (2014). The Role of SGLT1 and GLUT2 in Intestinal Glucose Transport and Sensing. *PLOS ONE* **9**, e89977.

Rodríguez-Piñeiro, A. M., Bergström, J. H., Ermund, A., Gustafsson, J. K., Schütte, A., Johansson, M. E. V. and Hansson, G. C. (2013). Studies of mucus in mouse stomach, small intestine, and colon. II. Gastrointestinal mucus proteome reveals Muc2 and Muc5ac accompanied by a set of core proteins. *American Journal of Physiology-Gastrointestinal and Liver Physiology* **305**, G348–G356.

Sala-Rabanal, M., Gallardo, M. A., Sánchez, J. and Planas, J. M. (2004). Na-dependent D-Glucose Transport by Intestinal Brush Border Membrane Vesicles from Gilthead Sea Bream (*Sparus aurata*). *The Journal of Membrane Biology* **201**, 85–96.

Sano, R., Shinozaki, Y. and Ohta, T. (2020). Sodium–glucose cotransporters: Functional properties and pharmaceutical potential. *Journal of Diabetes Investigation* **11**, 770–782.

Secor, S. M. and Diamond, J. (1995). Adaptive Responses to Feeding in Burmese Pythons: Pay Before Pumping. *Journal of Experimental Biology* **198**, 1313–1325.

Secor, S. M. and Diamond, J. (1998). A vertebrate model of extreme physiological regulation. *Nature* **395**, 659–662.

Smith., H. W. (1936). The Retention and Physiological Role of Urea in the Elasmobranchii. *Biological Reviews* **11**, 49–82.

Smith, K. M. and Baker, E. A. (2005). Characteristics of Spawning Lake Sturgeon in the Upper Black River, Michigan. *North American Journal of Fisheries Management* **25**, 301–307.

Smith, K. M. and King, D. K. (2005). Movement and Habitat Use of Yearling and Juvenile Lake Sturgeon in Black Lake, Michigan. *Transactions of the American Fisheries Society* **134**, 1159–1172.

Smolka, A. J., Lacy, E. R., Luciano, L. and Reale, E. (1994). Identification of gastric H,K-ATPase in an early vertebrate, the Atlantic stingray *Dasyatis sabina*. *Journal of Histochemistry and Cytochemistry* **42**, 1323–1332.

Sørensen, S. H., Norén, O., Sjöström, H. and Danielsen, E. M. (1982). Amphiphilic Pig Intestinal Microvillus Maltase/Glucoamylase. *European Journal of Biochemistry* **126**, 559–568.

Speers-Roesch, B. and Treberg, J. R. (2010). The unusual energy metabolism of elasmobranch fishes. *Comparative Biochemistry and Physiology Part A: Molecular & Integrative Physiology* **155**, 417–434.

Stöckli, J., Fazakerley, D. J. and James, D. E. (2011). GLUT4 exocytosis. *Journal of Cell Science* **124**, 4147–4159.

Stümpel, F., Burcelin, R., Jungermann, K. and Thorens, B. (2001). Normal kinetics of intestinal glucose absorption in the absence of GLUT2: Evidence for a transport pathway requiring glucose phosphorylation and transfer into the endoplasmic reticulum. *Proceedings of the National Academy of Sciences* **98**, 11330–11335.

Subramaniam, M., Weber, L. P. and Loewen, M. E. (2019). Intestinal electrogenic sodium-dependent glucose absorption in tilapia and trout reveal species differences in *SLC5A* -associated kinetic segmental segregation. *American Journal of Physiology-Regulatory, Integrative and Comparative Physiology* **316**, R222–R234.

Suzuki, T., Fujikura, K., Koyama, H., Matsuzaki, T., Takahashi, Y. and Takata, K. (2001). The apical localization of SGLT1 glucose transporter is determined by the short amino acid sequence in its N-terminal domain. *European Journal of Cell Biology* **80**, 765–774.

Syakuri, H., Adamek, M., Jung-Schroers, V., Matras, M., Reichert, M., Schröder, B., Breves, G. and Steinhagen, D. (2019). Glucose uptake in the intestine of the common carp *Cyprinus carpio*: Indications for the involvement of the sodium-dependent glucose cotransporter 1 and its modulation under pathogen infection. *Aquaculture* **501**, 169–177.

Teerijoki, H., Krasnov, A., Pitkänen, T. I. and Mölsä, H. (2001). Monosaccharide uptake in common carp (*Cyprinus carpio*) EPC cells is mediated by a facilitative glucose carrier.

Comparative Biochemistry and Physiology Part B: Biochemistry and Molecular Biology **128**, 483–491.

Theodosiou, N. A., Hall, D. A. and Jowdry, A. L. (2007). Comparison of acid mucin goblet cell distribution and Hox13 expression patterns in the developing vertebrate digestive tract. *Journal of Experimental Zoology Part B: Molecular and Developmental Evolution* **308B**, 442–453.

Theodosiou, N. A. and Oppong, E. (2019). 3D morphological analysis of spiral intestine morphogenesis in the little skate, *Leucoraja erinacea*. *Developmental Dynamics* **248**, 688–701.

Thorstensen, M. J., Weinrauch, A. M., Bugg, W. S., Jeffries, K. M. and Anderson, W. G. (2022). Tissue-specific transcriptomes reveal mechanisms of microbiome regulation in an ancient fish. *Database* **2023**, baad055.

Treberg, J. R., MacCormack, T. J., Lewis, J. M., Almeida-Val, V. M. F., Val, A. L. and Driedzic, W. R. (2007). Intracellular Glucose and Binding of Hexokinase and Phosphofructokinase to Particulate Fractions Increase under Hypoxia in Heart of the Amazonian Armored Catfish (*Liposarcus pardalis*). *Physiological and Biochemical Zoology* **80**, 542–550.

Uldry, M. and Thorens, B. (2004). The SLC2 family of facilitated hexose and polyol transporters. *Pflügers Archiv - European Journal of Physiology* **447**, 480–489.

Van Kempen, T. A. T. G. and Boerboom, G. M. (2023). Is the intestinal mucous layer a natural deep eutectic solvent-based digestion matrix? *American Journal of Physiology-Gastrointestinal and Liver Physiology* **324**, G438–G441.

Venero, J. A., Miles, R. D. and Chapman, F. A. (2015). Food Transit Time and Site of Absorption of Nutrients in Gulf of Mexico Sturgeon. *North American Journal of Aquaculture* **77**, 275–280.

Wegner, A., Ostaszewska, T. and Rożek, W. (2009). The ontogenetic development of the digestive tract and accessory glands of sterlet (*Acipenser ruthenus L.*) larvae during endogenous feeding. *Reviews in Fish Biology and Fisheries* **19**, 431.

Weinrauch, A. M., Clifford, A. M., Folkerts, E. J., Schaefer, C. M., Giacomin, M. and Goss, G. G. (2022a). Molecular identification and postprandial regulation of glucose carrier proteins in the

hindgut of Pacific hagfish, *Eptatretus stoutii*. *American Journal of Physiology-Regulatory, Integrative and Comparative Physiology* **322**, R336–R345.

Weinrauch, A. M., Clifford, A. M. and Goss, G. G. (2018). Functional redundancy of glucose acquisition mechanisms in the hindgut of Pacific hagfish (*Eptatretus stoutii*). *Comparative Biochemistry and Physiology Part A: Molecular & Integrative Physiology* **216**, 8–13.

Weinrauch, A. M., Fehrmann, F. and Anderson, W. G. (2022b). Sustained endocrine and exocrine function in the pancreas of the Pacific spiny dogfish post-feeding. *Fish Physiology Biochemistry* **48**, 645–657.

Wilson, R. P. (1994). Utilization of dietary carbohydrate by fish. *Aquaculture* **124**, 67–80.

Wilson, J. M. and Castro, L. F. C. (2010). 1 - Morphological diversity of the gastrointestinal tract in fishes. In *Fish Physiology* (ed. Grosell, M., Farrell, A. P., and Brauner, C. J.), pp. 1–55. Academic Press.

Wimmer, B., Raja, M., Hinterdorfer, P., Gruber, H. J. and Kinne, R. K.-H. (2009). C-terminal Loop 13 of Na+/Glucose Cotransporter 1 Contains Both Stereospecific and Non-stereospecific Sugar Interaction Sites. *Journal of Biological Chemistry* **284**, 983–991.

Wood, C. M., Kajimura, M., Bucking, C. and Walsh, P. J. (2007). Osmoregulation, ionoregulation and acid–base regulation by the gastrointestinal tract after feeding in the elasmobranch (*Squalus acanthias*). *Journal of Experimental Biology* **210**, 1335–1349.

Wright, E. M., Ghezzi, C. and Loo, D. D. F. (2017). Novel and Unexpected Functions of SGLTs. *Physiology (Bethesda)* **32**, 435–443.

Wright, E. M., Martín, M. G. and Turk, E. (2003). Intestinal absorption in health and disease—sugars. *Best Practice & Research Clinical Gastroenterology* **17**, 943–956.

Wright, E. M. and Turk, E. (2004). The sodium/glucose cotransport family SLC5. *Pflügers Archiv - European Journal of Physiology* **447**, 510–518.

Wright, P. A. and Wood, C. M. (2015). 5 - Regulation of Ions, Acid–Base, and Nitrogenous Wastes in Elasmobranchs. In *Fish Physiology* (ed. Shadwick, R. E., Farrell, A. P., and Brauner, C. J.), pp. 279–345. Academic Press.

Yoshida, A., Takata, K., Kasahara, T., Aoyagi, T., Saito, S. and Hirano, H. (1995). Immunohistochemical localization of Na+-dependent glucose transporter in the rat digestive tract. *Journal of Histochemistry & Cytochemistry* **27**, 420–426.

Yoshikawa, T., Inoue, R., Matsumoto, M., Yajima, T., Ushida, K. and Iwanaga, T. (2011). Comparative expression of hexose transporters (SGLT1, GLUT1, GLUT2 and GLUT5) throughout the mouse gastrointestinal tract. *Histochemistry and Cell Biology* **135**, 183–194.

Zeuthen, T., Gorraitz, E., Her, K., Wright, E. M. and Loo, D. D. F. (2016). Structural and functional significance of water permeation through cotransporters. *Proceedings of the National Academy of Sciences* **113**, E6887–E6894.

Zhang, Y., Qin, C., Yang, L., Lu, R., Zhao, X. and Nie, G. (2018). A comparative genomics study of carbohydrate/glucose metabolic genes: from fish to mammals. *BMC Genomics* **19**, 246.